Lecture Notes for the Course in Water Wave Mechanics

Andersen, Thomas Lykke; Frigaard, Peter

Publication date:
2011

Document Version
Publisher's PDF, also known as Version of record

LECTURE NOTES FOR THE COURSE IN
WATER WAVE MECHANICS

Thomas Lykke Andersen & Peter Frigaard

ISSN 1901-7286
DCE Lecture Notes No. 24

AALBORG UNIVERSITY
Department of Civil Engineering

Aalborg University
Department of Civil Engineering
Water and Soil

DCE Lecture Notes No. 24

LECTURE NOTES FOR THE COURSE IN WATER WAVE MECHANICS

by

Thomas Lykke Andersen & Peter Frigaard

July 2011

Scientific Publications at the Department of Civil Engineering

Technical Reports are published for timely dissemination of research results and scientific work carried out at the Department of Civil Engineering (DCE) at Aalborg University. This medium allows publication of more detailed explanations and results than typically allowed in scientific journals.

Technical Memoranda are produced to enable the preliminary dissemination of scientific work by the personnel of the DCE where such release is deemed to be appropriate. Documents of this kind may be incomplete or temporary versions of papers—or part of continuing work. This should be kept in mind when references are given to publications of this kind.

Contract Reports are produced to report scientific work carried out under contract. Publications of this kind contain confidential matter and are reserved for the sponsors and the DCE. Therefore, Contract Reports are generally not available for public circulation.

Lecture Notes contain material produced by the lecturers at the DCE for educational purposes. This may be scientific notes, lecture books, example problems or manuals for laboratory work, or computer programs developed at the DCE.

Theses are monograms or collections of papers published to report the scientific work carried out at the DCE to obtain a degree as either PhD or Doctor of Technology. The thesis is publicly available after the defence of the degree.

Latest News is published to enable rapid communication of information about scientific work carried out at the DCE. This includes the status of research projects, developments in the laboratories, information about collaborative work and recent research results.

First published December 2008

Second edition published 2011 by
Aalborg University
Department of Civil Engineering
Sohngaardsholmsvej 57,
DK-9000 Aalborg, Denmark

Printed in Denmark at Aalborg University

ISSN 1901-7286 DCE Lecture Notes No. 24

Preface

The present notes are written for the course in water wave mechanics given on the 7th semester of the education in civil engineering at Aalborg University.

The prerequisites for the course are the course in fluid dynamics also given on the 7th semester and some basic mathematical and physical knowledge. The course is at the same time an introduction to the course in coastal hydraulics on the 8th semester. The notes cover the following five lectures:

- Definitions. Governing equations and boundary conditions. Derivation of velocity potential for linear waves. Dispersion relationship.
- Particle paths, velocities, accelerations, pressure variation, deep and shallow water waves, wave energy and group velocity.
- Shoaling, refraction, diffraction and wave breaking.
- Irregular waves. Time domain analysis of waves.
- Wave spectra. Frequency domain analysis of waves.

The present notes are based on the following existing notes and books:

- H.F.Burcharth: Bølgehydraulik, AaU (1991)
- H.F.Burcharth og Torben Larsen: Noter i bølgehydraulik, AaU (1988).
- Peter Frigaard and Tue Hald: Noter til kurset i bølgehydraulik, AaU (2004)
- Zhou Liu and Peter Frigaard: Random Seas, AaU (1997)
- Ib A.Svendsen and Ivar G.Jonsson: Hydrodynamics of Coastal Regions, Den private ingeniørfond, DtU.(1989).
- Leo H. Holthuijsen: Waves in ocean and coastal waters, Cambridge University Press (2007).

Contents

Chapter 1

Phenomena, Definitions and Symbols

1.1 Wave Classification

Various types of waves can be observed at the sea that generally can be divided into different groups depending on their frequency and the generation method.

Phenomenon	Origin	Period
Surges	Atmospheric pressure and wind	1 – 30 days
Tides	Gravity forces from the moon and the sun	app. 12 and 24 h
Barometric wave	Air pressure variations	1 – 20 h
Tsunami	Earthquake, submarine land slide or submerged volcano	5 – 60 min.
Seiches (water level fluctuations in bays and harbour basins)	Resonance of long period wave components	1 – 30 min.
Surf beat, mean water level fluctuations at the coast	Wave groups	0.5 – 5 min.
Swells	Waves generated by a storm some distance away	$<$ 40 sec.
Wind generated waves	Wind shear on the water surface	$<$ 25 sec.

The phenomena in the first group are commonly not considered as waves, but as slowly changes of the mean water level. These phenomena are therefore also characterized as water level variations and are described by the mean water level MWL.

In the following is only considered short-period waves. Short-period waves are wind generated waves with periods less than approximately 40 seconds. This group of waves includes also for danish waters the most important phenomena.

1.2 Description of Waves

Wind generated waves starts to develop at wind speeds of approximately 1 m/s at the surface, where the wind energy is partly transformed into wave energy by surface shear. With increasing wave height the wind-wave energy transformation becomes even more effective due to the larger roughness.

A wind blown sea surface can be characterized as a very irregular surface, where waves apparently continuously arise and disappear. Smaller ripples are superimposed on larger waves and the waves travel with different speed and partly also different direction. A detailed description seems impossible and it is necessary to make some simplifications, which makes it possible to describe the larger changes in characteristics of the wave pattern.

Waves are classified into one of the following two classes depending on their directional spreading:

Long-crested waves:	2-dimensional (plane) waves (e.g. swells at mild sloping coasts). Waves are long crested and travel in the same direction (e.g. perpendicular to the coast)
Short-crested waves:	3-dimensional waves (e.g. wind generated storm waves). Waves travel in different directions and have a relative short crest.

In the rest of these notes only long-crested (2D) waves are considered, which is a good approximation in many cases. However, it is important to be aware that in reality waves are most often short-crested, and only close to the coast the waves are close to be long crested. Moreover, the waves are in the present note described using the linear wave theory, the so-called Stokes 1. order theory. This theory is only valid for low steepness waves in relative deep water.

1.3 Definitions and Symbols

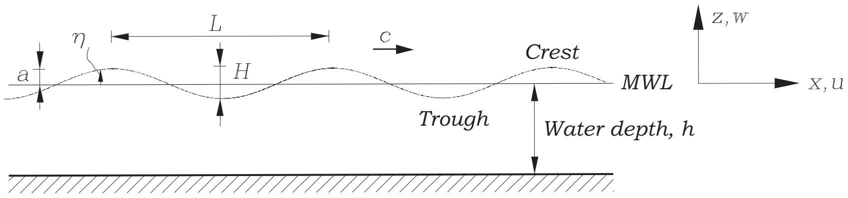

H	wave height
a	wave amplitude
η	water surface elevations from MWL (posituve upwards)
L	wave length
$s = \dfrac{H}{L}$	wave steepness
$c = \dfrac{L}{T}$	phase velocity of wave
T	wave period, time between two crests passage of same vertical section
u	horizontal particle velocity
w	vertical particle velocity
$k = \dfrac{2\pi}{L}$	wave number
$\omega = \dfrac{2\pi}{T}$	cyclic frequency, angular frequency
h	water depth

Wave fronts

Wave orthogonals

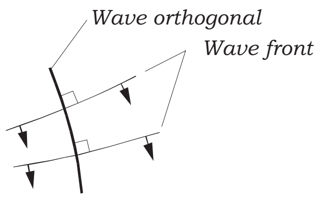

Chapter 2

Governing Equations and Boundary Conditions

In the present chapter the basic equations and boundary conditions for plane and regular surface gravity waves on constant depth are given. An analytical solution of the problem is found to be impossible due to the non-linear boundary conditions at the free surface. The governing equations and the boundary conditions are identical for both linear and higher order Stokes waves, but the present note covers only the linear wave theory, where the boundary conditions are linearized so an analytical solution is possible, cf. chapter 3.

We will start by analysing the influence of the bottom boundary layer on the ambient flow. Afterwards the governing equations and the boundary conditions will be discussed.

2.1 Bottom Boundary Layer

It is well known that viscous effects are important in boundary layers flows. Therefore, it is important to consider the bottom boundary layer for waves the effects on the flow outside the boundary layer. The observed particle motions in waves are given in Fig. 2.1. In a wave motion the velocity close to the bottom is a horizontal oscillation with a period equal to the wave period. The consequence of this oscillatory motion is the boundary layer always will remain very thin as a new boundary layer starts to develop every time the velocity changes direction.

As the boundary layer is very thin dp/dx is almost constant over the boundary layer. As the velocity in the boundary layer is smaller than in the ambient flow the particles have little inertia reacts faster on the pressure gradient. That is the reason for the velocity change direction earlier in the boundary layer than in the ambient flow. A consequence of that is the boundary layer seems to be moving away from the wall and into the ambient flow (separation of the boundary layer). At the same time a new boundary starts to develop.

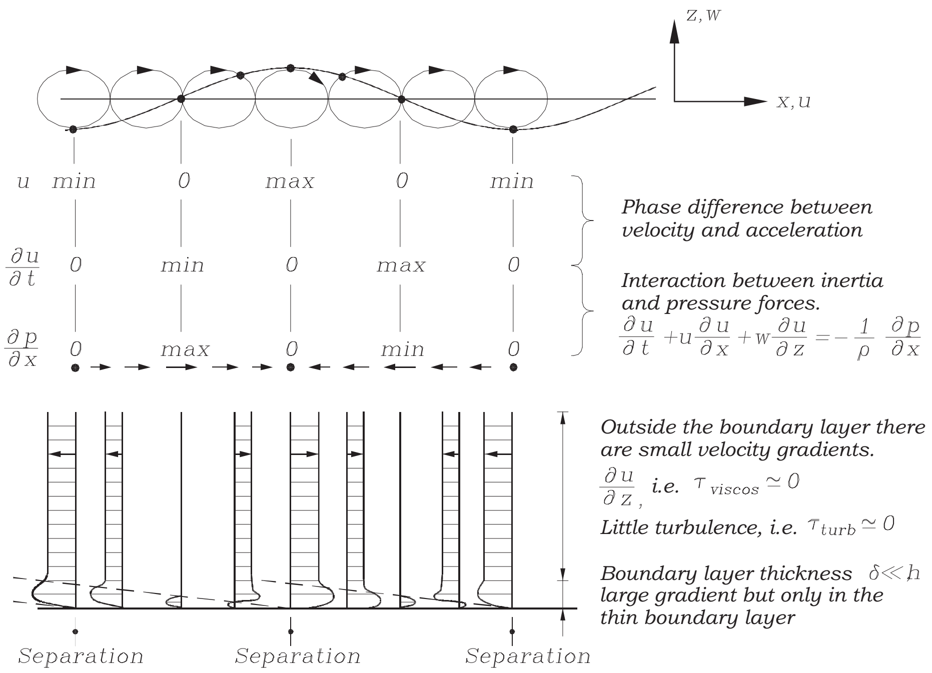

Figure 2.1: Observed particle motions in waves.

In the boundary layer is generated vortices that partly are transported into the ambient flow. However, due to the oscillatory flow a large part of the vortices will be destroyed during the next quarter of the wave cycle. Therefore, only a very small part of the generated vortices are transported into the ambient wave flow and it can be concluded that the boundary layer does almost not affect the ambient flow.

The vorticity which often is denoted $rot\vec{v}$ or $curl\vec{v}$ is in the boundary layer: $rot\vec{v} = \frac{\partial u}{\partial z} - \frac{\partial w}{\partial x} \simeq \frac{\partial u}{\partial z}$, as $w \simeq 0$ and hence $\frac{\partial w}{\partial x} \simeq 0$. $\frac{\partial u}{\partial z}$ is large in the boundary layer but changes sign twice for every wave period. Therefore, inside the boundary layer the flow has vorticity and the viscous effects are important. Outside the boundary layer the flow is assumed irrotational as:

> The viscous forces are neglectable and the external forces are essentially conservative as the gravitation force is dominating. Therefore, we neglect surface tension, wind-induced pressure and shear stresses and the Coriolis force. This means that if we consider waves longer than a few centimeters and shorter than a few kilometers we can assume that the external forces are conservative. As

a consequence of that and the assumption of an inviscid fluid, the vorticity is constant cf. Kelvin's theorem. As $rot\vec{v} = 0$ initially, this will remain the case.

The conclusion is that the ambient flow (the waves) with good accuracy could be described as a *potential flow*.

The velocity potential is a function of x, z and t, $\varphi = \varphi(x, z, t)$. Note that both $\varphi(x, z, t)$ and $\varphi(x, z, t) + f(t)$ will represent the same velocity field (u, w), as $\left(\frac{\partial\varphi}{\partial x}\ ,\ \frac{\partial\varphi}{\partial z}\right)$ is identical. However, the reference for the pressure is different.

With the introduction of φ the number of variables is reduced from three (u, w, p) to two (φ, p).

2.2 Governing Hydrodynamic Equations

From the theory of fluid dynamics the following basic balance equations are taken:

Continuity equation for plane flow and incompresible fluid with constant density (mass balance equation)

$$\frac{\partial u}{\partial x} + \frac{\partial w}{\partial z} = 0 \quad \text{or} \quad div\,\vec{v} = 0 \tag{2.1}$$

The assumption of constant density is valid in most situations. However, vertical variations may be important in some special cases with large vertical differences in temperature or salinity. Using the continuity equation in the present form clearly reduces the validity to non-breaking waves as wave breaking introduces a lot of air bubbles in the water and in that case the body is not continuous.

Laplace-equation (plane irrotational flow)
In case of irrotational flow Eq. 2.1 can be expressed in terms of the velocity potential φ and becomes the Laplace equation as $v_i = \frac{\partial\varphi}{\partial x_i}$.

$$\frac{\partial^2\varphi}{\partial x^2} + \frac{\partial^2\varphi}{\partial z^2} = 0 \tag{2.2}$$

Equations of motions (momentum balance)
Newton's 2. law for a *particle* with mass m with external forces $\sum \overline{K}$ acting on the particle is, $m\,\frac{d\vec{v}}{dt} = \sum \overline{K}$. The general form of this is the Navier-Stoke

equations which for an ideal fluid (inviscid fluid) can be reduced to the Euler equations as the viscous forces can be neglected.

$$\rho \frac{d\vec{v}}{dt} = -grad\, p + \rho \vec{g} \quad (+ \text{ viscous forces}) \tag{2.3}$$

Bernoulli's generalized equation (plane irrotational flow)
In case of irrotational flow the Euler equations can be rewritten to get the generalized Bernoulli equation which is an integrated form of the equations of motions.

$$g\, z + \frac{p}{\rho} + \frac{1}{2}\left(u^2 + w^2\right) + \frac{\partial \varphi}{\partial t} = C(t)$$

$$g\, z + \frac{p}{\rho} + \frac{1}{2}\left(\left(\frac{\partial \varphi}{\partial x}\right)^2 + \left(\frac{\partial \varphi}{\partial z}\right)^2\right) + \frac{\partial \varphi}{\partial t} = C(t) \tag{2.4}$$

Note that the velocity field is independent of $C(t)$ but the reference for the pressure will depend on $C(t)$.

Summary on system of equations:
Eq. 2.2 and 2.4 is two equations with two unknowns (φ, p). Eq. 2.2 can be solved separately if only $\varphi = \varphi(x, z, t)$ and not $p(x, z, t)$ appear explicitly in the boundary conditions. This is usually the case, and we are left with $\varphi(x, z, t)$ as the only unknown in the governing Laplace equation. Hereafter, the pressure $p(x, z, t)$ can be found from Eq. 2.4. Therefore, the pressure p can for potential flows be regarded as a reaction on the already determined velocity field. A reaction which in every point obviously must fulfill the equations of motion (Newton's 2. law).

2.3 Boundary Conditions

Based on the previous sections we assume incompressible fluid and irrotational flow. As the Laplace equation is the governing differential equation for all potential flows, the character of the flow is determined by the boundary conditions. The boundary conditions are of kinematic and dynamic nature. The kinematic boundary conditions relate to the motions of the water particles while the dynamic conditions relate to forces acting on the particles. Free surface flows require one boundary condition at the bottom, two at the free surface and boundary conditions for the lateral boundaries of the domain.

I case of waves the lateral boundary condition is controlled by the assumption that the waves are periodic and long-crested. The boundary conditions at the free surface specify that a particle at the surface remains at the surface (kinematic) and that the pressure is constant at the surface (dynamic) as wind induced pressure variations are not taken into account. In the following the mathematical formulation of these boundary conditions is discussed. The boundary condition at the bottom is that there is no flow flow through the bottom (vertical velocity component is zero). As the fluid is assumed ideal (no friction) there is not included a boundary condition for the horizontal velocity at the bottom.

2.3.1 Kinematic Boundary Condition at Bottom

Vertical velocity component is zero as there should not be a flow through the bottom:

$$w = 0 \;\text{ or }\; \frac{\partial \varphi}{\partial z} = 0 \quad \text{for } z = -h \tag{2.5}$$

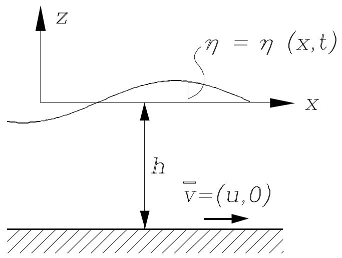

2.3.2 Boundary Conditions at the Free Surface

One of the two surface conditions specify that a particle at the surface remains at the surface (kinematic boundary condition). This *kinematic boundary condition* relates the vertical velocity of a particle at the surface to the vertical velocity of the surface, which can be expressed as:

$$\begin{aligned} w &= \frac{d\eta}{dt} = \frac{\partial \eta}{\partial t} + \frac{\partial \eta}{\partial x}\frac{dx}{dt} = \frac{\partial \eta}{\partial t} + \frac{\partial \eta}{\partial x} u \quad , \quad \text{or} \\ \frac{\partial \varphi}{\partial z} &= \frac{\partial \eta}{\partial t} + \frac{\partial \eta}{\partial x}\frac{\partial \varphi}{\partial x} \qquad \text{for} \quad z = \eta \end{aligned} \tag{2.6}$$

The following figure shows a geometrical illustration of this problem.

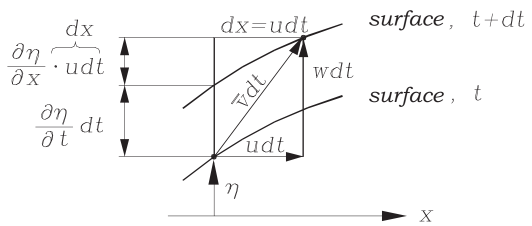

The second surface condition specifies the pressure at free surface (dynamic boundary condition). This *dynamic condition* is that the pressure along the surface must be equal to the atmospheric pressure as we disregard the influence of the wind. We assume the atmospheric pressure p_0 is constant which seems valid as the variations in the pressure are of much larger scale than the wave length, i.e. the pressure is only a function of time $p_0 = p_0(t)$. If this is inserted into Eq. 2.4, where the right hand side exactly express a constant pressure divided by mass density, we get:

$$g\,z + \frac{p}{\rho} + \frac{1}{2}\left(u^2 + w^2\right) + \frac{\partial\varphi}{\partial t} = \frac{p_0}{\rho}$$

At the surface $z = \eta$ we have $p = p_0$ and above can be rewritten as the boundary condition:

$$g\eta + \frac{1}{2}\left(\left(\frac{\partial\varphi}{\partial x}\right)^2 + \left(\frac{\partial\varphi}{\partial z}\right)^2\right) + \frac{\partial\varphi}{\partial t} = 0 \qquad \text{for } z = \eta \tag{2.7}$$

The same result can be found from Eq. 2.4 by setting p equal to the excess pressure relative to the atmospheric pressure.

2.3.3 Boundary Condition Reflecting Constant Wave Form (Periodicity Condition)

The *periodicity condition* reflects that the wave is a *periodic, progressive wave of constant form*. This means that the wave propagate with constant form in the positive x-direction. The consequence of that is the flow field must be identical in two sections separated by an integral number of wave lengths. This sets restrictions to the variation of η and φ (i.e. surface elevation and velocity field) with t and x (i.e. time and space).

The requirement of constant form can be expressed as:

$$\eta(x,t) = \eta(x + nL, t) = \eta(x, t + nT) \ , \quad \text{where } n = 1, 2, 3, \ldots$$

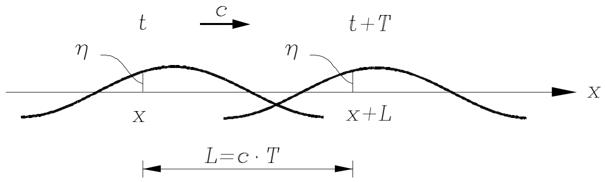

This criteria is fulfilled if (x,t) is combined in the variable $\left(L\,\frac{t}{T} - x\right)$, as $\eta\left(L\,\frac{t}{T} - x\right) = \eta\left(L\,\frac{(t+nT)}{T} - (x + nL)\right) = \eta\left(L\,\frac{t}{T} - x\right)$. This variable can be expressed in dimensionless form by dividing by the wave length L. $\frac{2\pi}{L}\left(L\,\frac{t}{T} - x\right) = 2\pi\left(\frac{t}{T} - \frac{x}{L}\right)$, where the factor 2π is added due to the following calculations.

We have thus included the periodicity condition for η and φ by introducing the variable θ.

$$\eta = \eta(\theta) \quad \text{and} \quad \varphi = \varphi(\theta, z) \quad \text{where } \theta = 2\pi\left(\frac{t}{T} - \frac{x}{L}\right) \tag{2.8}$$

If we introduce the wave number $k = \frac{2\pi}{L}$ and the cyclic frequency $\omega = \frac{2\pi}{T}$ we get:

$$\theta = \omega t - kx \tag{2.9}$$

It is now verified that Eqs. 2.8 and 2.9 corresponds to a wave propagating in the positive x-direction, i.e. for a given value of η should x increase with time t. Eq. 2.9 can be rewritten to:

$$x = \frac{1}{k}(\omega t - \theta)$$

From which it can be concluded that x increases with t for a given value of θ. If we change the sign of the kx term form minus to plus the wave propagation direction changes to be in the negative x-direction.

2.4 Summary of Mathematical Problem

The governing Laplace equation and the boundary conditions (BCs) can be summarized as:

$$\text{Laplace equation} \quad \frac{\partial^2 \varphi}{\partial x^2} + \frac{\partial^2 \varphi}{\partial z^2} = 0 \tag{2.10}$$

$$\text{Kin. bottom BC} \quad \frac{\partial \varphi}{\partial z} = 0 \quad \text{for} \ \ z = -h \tag{2.11}$$

$$\text{Kin. surface BC} \quad \frac{\partial \varphi}{\partial z} = \frac{\partial \eta}{\partial t} + \frac{\partial \eta}{\partial x}\frac{\partial \varphi}{\partial x} \quad \text{for} \ \ z = \eta \tag{2.12}$$

$$\text{Dyn. surface BC} \quad g\eta + \frac{1}{2}\left(\left(\frac{\partial \varphi}{\partial x}\right)^2 + \left(\frac{\partial \varphi}{\partial z}\right)^2\right) + \frac{\partial \varphi}{\partial t} = 0 \quad \text{for } z = \eta \tag{2.13}$$

$$\text{Periodicity BC} \quad \begin{array}{l} \eta(x,t) \text{ and } \varphi(x,z,t) \Rightarrow \\ \eta(\theta) \ , \ \varphi(\theta, z) \\ \text{where } \theta = \omega t - kx \end{array}$$

An analytical solution to the problem is impossible. This is due to the two mathematical difficulties:

- Both boundary conditions at the free surface are non-linear.
- The shape and position of the free surface η is one of the unknowns of the problem that we try to solve which is not included in the governing Laplace equation, Eq. 2.10. Therefore, a governing equation with η is missing.

A matematical simplification of the problem is needed.

Chapter 3

Linear Wave Theory

The linear wave theory which is also known as the Airy wave theory (Airy, 1845) or Stokes 1. order theory (Stokes, 1847), is described in the present chapter and the assumptions made are discussed. Based on this theory analytical expressions for the particle velocities, particle paths, particle accelerations and pressure are established.

The linear theory is strictly speaking only valid for non-breaking waves with small amplitude, i.e. when the amplitude is small compared to the wave length and the water depth (H/L and H/h are small). However, the theory is fundamental for understanding higher order theories and for the analysis of irregular waves, cf. chapter 5. Moreover, the linear theory is the simplest possible case and turns out also to be the least complicated theory.

By assuming $H/L << 1$, i.e. small wave steepness, it turns out that the boundary conditions can be linearized and η can be eliminated from the equations. This corresponds to the surface conditions can be taken at $z = 0$ instead of $z = \eta$ and the differential equation can be solved analytically. The linearisation of the boundary conditions is described in the following section.

3.1 Linearisation of Boundary Conditions

The two surface boundary conditions (Eqs. 2.12 and 2.13) are the two non-linear conditions that made an analytical solution to the problem impossible. These are linearised in the following by investigating the importance of the various terms.

3.1.1 Linearisation of Kinematic Surface Condition

The non-linearised kinematic surface condition is, cf. Eq. 2.12:

$$\frac{\partial \varphi}{\partial z} = \frac{\partial \eta}{\partial t} + \frac{\partial \eta}{\partial x}\frac{\partial \varphi}{\partial x} \quad for \;\; z = \eta \tag{3.1}$$

The magnitude of the different terms is investigated in the following, where σ indicate the order of magnitude. If we consider a deep water wave ($H/h << 1$) observations has shown that the particle paths are circular and as the particles on the surface must remain on the surface the diameter in the circular motion must close to the surface be equal to the wave height H. As the duration of each orbit is equal to the wave period T, the speed of the particles close to the surface can be approximated by $\pi H/T$.

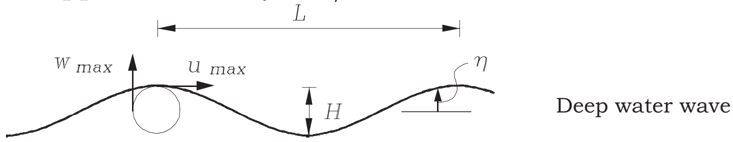

$$
\begin{aligned}
max\frac{\partial \varphi}{\partial x} &= u_{max} = \frac{\pi H}{T} = \sigma\left(\frac{H}{T}\right) \\
max\frac{\partial \varphi}{\partial z} &= w_{max} = \frac{\pi H}{T} = \sigma\left(\frac{H}{T}\right) \\
\frac{\partial \eta}{\partial x} &= \sigma\left(\frac{H}{L}\right) \quad \text{, as } \eta \text{ varies } H \text{ over the length } L/2 \\
\frac{\partial \eta}{\partial t} &= \sigma\left(\frac{H}{T}\right) \quad \text{, as } \eta \text{ varies } H \text{ over the time } T/2
\end{aligned}
$$

Therefore, we get from Eq. 3.1:

$$\sigma\left(\frac{H}{T}\right) = \sigma\left(\frac{H}{T}\right) + \sigma\left(\frac{H}{L}\right)\sigma\left(\frac{H}{T}\right)$$

from which it can be seen that the order of magnitude of the last non-linear term is H/L smaller than the order of the linear term. As we assumed $\frac{H}{L} << 1$ we only make a small error by neglecting the non-linear term. However, the argumentation can be risky as we have not said anything about the simoultanousness of the maximum values of each term.

The linaerised kinematic surface boundary condition is thus:

$$\frac{\partial \varphi}{\partial z} = \frac{\partial \eta}{\partial t} \quad , \quad \text{for} \quad z = \eta \tag{3.5}$$

However, we still have the problem that the boundary condition is expressed at $z = \eta$ as the position of the surface is unknown. An additional simplificaion is needed. $\frac{\partial \varphi}{\partial z}$, which is the only term in Eq. 3.5 that depends on z, is expanded in a Taylor series to evaluate the posibilities to discard higher order terms. The general form of the Taylor series is:

$$f(z + \Delta z) = f(z) + \frac{\Delta z}{1!} f'(z) + \frac{(\Delta z)^2}{2!} f''(z) + \ldots + \frac{(\Delta z)^n}{n!} f^{(n)}(z) + R_n(z)$$

where Δz represent a deviation from the variable z. With the Taylor expansion we can get any preassigned accuracy in the approximation of $f(z + \Delta z)$ by choosing n large enough. We now make a Taylor series expansion of $\frac{\partial\varphi}{\partial z}$ from $z=0$ to calculate the values at $z=\eta$, i.e. we set $\Delta z=\eta$ and get:

$$\begin{aligned}\frac{\partial\varphi}{\partial z}(x,\eta,t) &= \frac{\partial\varphi}{\partial z}(x,0,t)+\frac{\eta}{1!}\frac{\partial^2\varphi(x,0,t)}{\partial z^2}+\dots\\ &= \frac{\partial\varphi}{\partial z}(x,0,t)+\frac{\eta}{1!}\left(\frac{-\partial^2\varphi(x,0,t)}{\partial x^2}\right)+\dots\end{aligned}\tag{3.6}$$

where $\frac{\partial^2\varphi}{\partial x^2}+\frac{\partial^2\varphi}{\partial z^2}=0$ has been used.

As $\eta=\sigma(H)$ and $\frac{\partial^2\varphi}{\partial x^2}=\sigma\left(\frac{1}{L}\frac{\partial\varphi}{\partial x}\right)=\sigma\left(\frac{1}{L}\frac{\partial\varphi}{\partial z}\right)$, as $u=\sigma(w)$, we get from Eq. 3.6:

$$\frac{\partial\varphi}{\partial z}(x,\eta,t)=\frac{\partial\varphi}{\partial z}(x,0,t)+\overbrace{\sigma(H)\sigma\left(\frac{-1}{L}\frac{\partial\varphi}{\partial z}\right)}^{\sigma\left(\frac{H}{L}\frac{\partial\varphi}{\partial z}\right)}\simeq\frac{\partial\varphi}{\partial z}(x,0,t)\ ,\ \text{as}\ \frac{H}{L}<<1.$$

The use of $z=0$ instead of $z=\eta$ in Eqs. 3.1 and 3.5 corresponds thus to neglecting the small second order term with the same magnitude as the non-linear term in the boundary condition removed above. The *linearised kinematic surface boundary condition* is therefore simplified to:

$$\frac{\partial\varphi}{\partial z}=\frac{\partial\eta}{\partial t}\qquad\text{for } z=0\tag{3.7}$$

The error committed by evaluating φ at MWL ($z=0$) instead of at the surface ($z=\eta$) is thus small and of second order.

3.1.2 Linearisation of Dynamic Surface Condition

The non-linaerised dynamic surface boundary condition reads, cf. Eq. 2.13:

$$g\eta+\frac{1}{2}\left(\left(\frac{\partial\varphi}{\partial x}\right)^2+\left(\frac{\partial\varphi}{\partial z}\right)^2\right)+\frac{\partial\varphi}{\partial t}=0\qquad\text{for}\quad z=\eta\tag{3.8}$$

The linearisation of the dynamic surface boundary condition follows the same approach as for the kinematic condition. We start by examining the magnitude of the different terms. For the assessment of the magnitude of the term $\frac{\partial\varphi}{\partial t}$, is used $\frac{\partial}{\partial x}\left(\frac{\partial\varphi}{\partial t}\right)=\frac{\partial}{\partial t}\left(\frac{\partial\varphi}{\partial x}\right)=\frac{\partial u}{\partial t}$ i.e. $\frac{\partial}{\partial x}\left(\frac{\partial\varphi}{\partial t}\right)=\sigma\left(\frac{1}{L}\frac{\partial\varphi}{\partial t}\right)=\frac{\partial u}{\partial t}=\sigma\left(\frac{H/T}{T}\right)$, as $u=\sigma\left(\frac{H}{T}\right)$.

Therefore, we get:

$$\frac{\partial\varphi}{\partial t}=\sigma\left(L\frac{H}{T^2}\right)\tag{3.9}$$

Moreover we have for the quadratic terms:

$$\left(\frac{\partial \varphi}{\partial x}\right)^2 \simeq \left(\frac{\partial \varphi}{\partial z}\right)^2 = \sigma\left(\frac{H}{T}\right)^2 = \sigma\left(L\,\frac{H}{T^2}\right)\sigma\left(\frac{H}{L}\right) = \sigma\left(\frac{\partial \varphi}{\partial t}\cdot\frac{H}{L}\right)$$

From this we can conclude that the quadratic terms are small and of higher order and as a consequence they are neglected. Therefore, we can in case of small amplitude waves write the boundary condition as:

$$g\eta + \frac{\partial \varphi}{\partial t} = 0 \qquad \text{for} \quad z = \eta \tag{3.10}$$

However, the problem with the unknown position of the free surface (η) still exists. We use a Taylor expansion of $\frac{\partial \varphi}{\partial t}$ around $z = 0$, which is the only term in Eq. 3.10 that depends on z.

$$\frac{\partial \varphi}{\partial t}(x,\eta,t) = \frac{\partial \varphi}{\partial t}(x,0,t) + \frac{\eta}{1!}\frac{\partial}{\partial z}\left(\frac{\partial \varphi}{\partial t}(x,0,t)\right) + \ldots \tag{3.11}$$

$$\frac{\partial \varphi}{\partial t} = \sigma\left(L\,\frac{H}{T^2}\right) \text{ cf. eq. 3.9,}$$

$$\eta\,\frac{\partial}{\partial z}\left(\frac{\partial \varphi}{\partial t}\right) = \eta\,\frac{\partial}{\partial t}\left(\frac{\partial \varphi}{\partial z}\right) = \sigma(H)\,\sigma\left(\frac{1}{T}\,\frac{\partial \varphi}{\partial z}\right) =$$

$$\sigma(H)\,\sigma\left(\frac{1}{T}\right)\,\sigma\left(\frac{H}{T}\right) = \sigma\left(\frac{H^2}{T^2}\right) = \sigma\left(\frac{H}{L}\right)\,\sigma\left(L\,\frac{H}{T^2}\right) \text{ which is}$$

$$\sigma\left(\frac{H}{L}\,\frac{\partial \varphi}{\partial t}\right) \text{ i.e. } << \frac{\partial \varphi}{\partial t}.$$

The second term in Eq. 3.11 is thus small and of higher order and can be neglected when $H/L << 1$. This corresponds to using $z = 0$ instead of $z = \eta$ in Eq. 3.10. As a consequence the *linearised dynamic surface boundary condition* is simplified to:

$$g\eta + \frac{\partial \varphi}{\partial t} = 0 \qquad \text{for} \quad z = 0 \tag{3.12}$$

3.1.3 Combination of Surface Boundary Conditions

The linearised surface boundary conditions Eqs. 3.7 and 3.12 are now combined in a single surface boundary condition. If we differentiate Eq. 3.12 with respect to t we get:

$$g\,\frac{\partial \eta}{\partial t} + \frac{\partial^2 \varphi}{\partial t^2} = 0 \qquad\qquad \text{for} \quad z = 0 \tag{3.13}$$

which can be rewritten as:

$$\frac{\partial \eta}{\partial t} = -\frac{1}{g}\frac{\partial^2 \varphi}{\partial t^2} \qquad \text{for} \quad z = 0 \tag{3.14}$$

This result is now inserted into Eq. 3.7 and we get the combined surface boundary condition:

$$\frac{\partial \varphi}{\partial z} + \frac{1}{g}\frac{\partial^2 \varphi}{\partial t^2} = 0 \qquad \text{for} \quad z = 0 \tag{3.15}$$

Now η has been eliminated from the boundary conditions and the mathematical problem is reduced enormously.

3.1.4 Summary of Linearised Problem

The mathematical problem can now be summarized as:

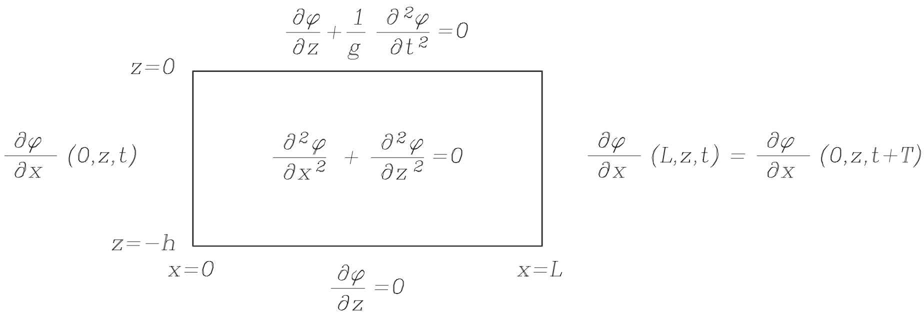

3.2 Inclusion of Periodicity Condition

The periodicity condition can as mentioned in section 2.3.3 by inclusion of θ given by Eq. 2.9 instead of the two variables (x, t). Therefore, the Laplace equation and the boundary conditions are rewritten to include $\varphi(\theta, z)$ instead of $\varphi(x, z, t)$. The coordinates are thus changed from (x, t) to (θ) by using the chain rule for differentiation and the definition $\theta = \omega t - kx$ (eq. 2.9).

$$\frac{\partial \varphi}{\partial x} = \frac{\partial \varphi}{\partial \theta}\frac{\partial \theta}{\partial x} = \frac{\partial \varphi}{\partial \theta}(-k) \tag{3.16}$$

$$\frac{\partial^2 \varphi}{\partial x^2} = \frac{\partial\left(\frac{\partial \varphi}{\partial x}\right)}{\partial x} = \frac{\partial\left(\frac{\partial \varphi}{\partial x}\right)}{\partial \theta}\frac{\partial \theta}{\partial x} = \frac{\partial\left(\frac{\partial \varphi}{\partial \theta}(-k)\right)}{\partial \theta}(-k) = k^2\frac{\partial^2 \varphi}{\partial \theta^2} \tag{3.17}$$

A similar approach for the time derivatives give:

$$\begin{aligned}\frac{\partial \varphi}{\partial t} &= \frac{\partial \varphi}{\partial \theta}\frac{\partial \theta}{\partial t} = \frac{\partial \varphi}{\partial \theta}\omega \\ \frac{\partial^2 \varphi}{\partial t^2} &= \omega^2\frac{\partial^2 \varphi}{\partial \theta^2}\end{aligned} \tag{3.18}$$

Eq. 3.17 is now inserted into the Laplace equation (Eq. 2.2) and we get:

$$k^2 \frac{\partial^2 \varphi}{\partial \theta^2} + \frac{\partial^2 \varphi}{\partial z^2} = 0 \tag{3.19}$$

Eq. 3.18 is inserted into Eq. 3.15 to get the free surface condition with θ included:

$$\frac{\partial \varphi}{\partial z} + \frac{\omega^2}{g} \frac{\partial^2 \varphi}{\partial \theta^2} = 0 \qquad \text{for} \quad z = 0 \tag{3.20}$$

The boundary condition at the bottom is unchanged ($\frac{\partial \varphi}{\partial z} = 0$).

The periodicity condition $\frac{\partial \varphi}{\partial x}\ (0, z, t) = \frac{\partial \varphi}{\partial x}\ (L, z, t)$ is changed by considering the values of θ for $x = 0$ and $x = L$:

For $x = 0$ and $t = t$ we get, $\theta = 2\pi \frac{t}{T}$.

For $x = L$ and $t = t$ — $\theta = 2\pi \frac{t}{T} - 2\pi$.

It can be shown that it is sufficient to to impose the periodicity condition on the horizontal velocity ($u = \frac{\partial \varphi}{\partial x}$), which yields by inclusion of Eq. 3.16:

$$-k \frac{\partial \varphi}{\partial \theta} \left(2\pi \frac{t}{T} \ , \ z \right) = -k \frac{\partial \varphi}{\partial \theta} \left(2\pi \frac{t}{T} - 2\pi \ , \ z \right) \ ,$$

which should be valid for all values of t and thus also for $t = 0$. As the periodicity condition could just as well been expressed for $x = -L$ instead of $x = L$ it can be concluded that the sign of 2π can be changed and we get:

$$-k \frac{\partial \varphi}{\partial \theta} (0, z) = -k \frac{\partial \varphi}{\partial \theta} (2\pi, z) \tag{3.21}$$

which is the reformulated periodicity condition.

3.3 Summary of Mathematical Problem

The mathematical problem from section 2.4 has now been enormously simplified by linearisation of the boundary conditions and inclusion of θ instead of x, t. The mathematical problem can now be solved analytically and summarized as:

$$\text{Laplace equation:} \qquad k^2 \frac{\partial^2 \varphi}{\partial \theta^2} + \frac{\partial^2 \varphi}{\partial z^2} = 0 \tag{3.22}$$

$$\text{Bottom BC:} \qquad \frac{\partial \varphi}{\partial z} = 0 \quad \text{for} \quad z = -h \tag{3.23}$$

$$\text{Linearised Surface BC:} \qquad \frac{\partial \varphi}{\partial z} + \frac{\omega^2}{g} \frac{\partial^2 \varphi}{\partial \theta^2} = 0 \quad \text{for} \quad z = 0 \tag{3.24}$$

$$\text{Periodicity BC:} \qquad -k \frac{\partial \varphi}{\partial \theta} (0, z) = -k \frac{\partial \varphi}{\partial \theta} (2\pi, z) \tag{3.25}$$

3.4 Solution of Mathematical Problem

The linear wave theory is based on an exact solution to the Laplace equation but with the use of linear approximations of the boundary conditions. The solution to the problem is straight forward and can be found by the method of separation of variables. Hence we introduce:

$$\varphi(\theta, z) = f(\theta) \cdot Z(z) \tag{3.26}$$

which inserted in Eq. 3.22 leads to:

$$k^2 f'' Z + Z'' f = 0$$

We then divide by $\varphi = fZ$ on both sides to get:

$$-k^2 \frac{f''}{f} = \frac{Z''}{Z} \tag{3.27}$$

As the left hand side now only depends on θ and the right hand only depends on z they must be equal to the same constant which we call λ^2 as the constant is assumed positive. Therefore, we get the following two differential equations:

$$f'' + \frac{\lambda^2}{k^2} f = 0 \tag{3.28}$$

$$Z'' - \lambda^2 Z = 0 \tag{3.29}$$

Eq. 3.28 has the solution:

$$f = A_1 cos\left(\frac{\lambda}{k}\theta\right) + A_2 sin\left(\frac{\lambda}{k}\theta\right) = A\, sin\left(\frac{\lambda}{k}\theta + \delta\right) \tag{3.30}$$

where A, λ and δ are constants to be determined from the boundary conditions. However, we can set δ equal to zero corresponding to an appropriate choice of the origin of $\theta = (x, t)$. Therefore, we can write:

$$f = A\, sin\left(\frac{\lambda}{k}\theta\right) \tag{3.31}$$

If we insert the definition in Eq. 3.26 into the periodicity condition (Eq. 3.25) we get the following condition:

$$f'(0) = f'(2\pi)$$

From Eq. 3.31 we get $f' = A\,\frac{\lambda}{k}\, cos\left(\frac{\lambda}{k}\theta\right)$ and hence the above condition gives:

$$A\frac{\lambda}{k} cos\left(\frac{\lambda}{k}0\right) = A\,\frac{\lambda}{k} = A\,\frac{\lambda}{k} cos\left(\frac{\lambda}{k}2\pi\right) \quad , \quad \text{i.e.}$$

$$\frac{\lambda}{k} = n \ , \quad \text{where} \ \ n = 1, 2, 3 \ldots \qquad\qquad (n \neq 0, \ \text{as} \ \lambda \neq 0)$$

This condition is now inserted into Eq. 3.31 and the solution becomes:

$$f = A \, sin(n\theta) = A \, sin\left(n\left(\omega t - \frac{2\pi}{L}\,x\right)\right)$$

As $x = L$ must correspond to one wave length we get $n = \frac{\lambda}{k} = 1$ as the only solution and $n = 2, 3, 4, ...$ must be disregarded. The result can also be written as $\lambda = k$ which is used later for the solution of the second differential equation. The result can also be obtained from $\theta = 2\pi$ by definition corresponds to one wave length. Therefore, we get the following solution to the f-function:

$$f = A \, sin\theta \tag{3.32}$$

The second differential equation, Eq. 3.29, has the solution:

$$Z = B_1 \, e^{\lambda z} + C_1 \, e^{-\lambda z} \tag{3.33}$$

As $sinh \, x = \frac{e^x - e^{-x}}{2}$ and $cosh \, x = \frac{e^x + e^{-x}}{2}$ and we choose $B_1 = \frac{B+C}{2}$ and $C_1 = \frac{B-C}{2}$ and at the same time introduce $\lambda = k$ as found above, we get:

$$Z = B \, cosh \, kz + C \, sinh \, kz \tag{3.34}$$

The three integration constants A, B and C left in Eqs. 3.32 and 3.34 are determined from the bottom and surface boundary conditions. We start by inserting Eq. 3.26 into the bottom condition (Eq. 3.23), $\frac{\partial \varphi}{\partial z} = 0$ for $z = -h$, and get:

$$Z' = 0 \quad \text{for} \ \ z = -h$$

We now differentiate Eq. 3.34 with respect to z and insert the above given condition:

$$B \, k \, sinh(-kh) + C \, k \, cosh(-kh) = 0 \quad \text{or} \quad B = C \, coth \, kh$$

as $sinh(-x) = -sinh(x)$, $cosh(-x) = cosh(x)$ and $coth(x) = \frac{cosh(x)}{sinh(x)}$.

This result is now inserted into Eq. 3.34 to get:

$$\begin{aligned} Z &= C \, (coth \, kh \, cosh \, kz + sinh \, kz) \\ &= \frac{C}{sinh \, kh} \, (cosh \, kh \, cosh \, kz + sinh \, kh \, sinh \, kz) \\ &= C \, \frac{cosh \, k(z+h)}{sinh \, kh} \end{aligned} \tag{3.35}$$

We now combine the solutions to the two differential equations by inserting Eqs. 3.32 and 3.35 into Eq. 3.26:

$$\varphi = f \cdot Z = AC\,\frac{cosh\,k(z+h)}{sinh\,kh}\,sin\theta \tag{3.36}$$

The product of the constants A and C is now determined from the linearised dynamic surface boundary condition (Eq. 3.12), $\eta = -\frac{1}{g}\frac{\partial\varphi}{\partial t}$ for $z = 0$, which express the surface form. We differentiate Eq. 3.36 with respect to t and insert the result into the dynamic surface condition to get:

$$\eta = -\frac{\omega}{g}\,AC\,\frac{cosh\,kh}{sinh\,kh}\,cos\theta \quad , \tag{3.37}$$

where $-\frac{\omega}{g}\,AC\,\frac{cosh\,kh}{sinh\,kh}$ must represent the wave amplitude $a \equiv \frac{H}{2}$. Therefore, the wave form must be given by:

$$\eta = a\,cos\theta = \frac{H}{2}\,cos(\omega t - kx) \tag{3.38}$$

The velocity potential is found by inserting the expression for AC and θ into Eq. 3.36:

$$\varphi = -\frac{a\,g}{\omega}\,\frac{cosh\,k\,(z+h)}{cosh\,kh}\,sin(\omega t - kx) \tag{3.39}$$

3.5 Dispersion Relationship

If we take a look on the velocity potential, Eq. 3.39, then we observe that the wave motion is specified by the four parameters a, ω, h and k or alternatively we can use the parameters H, T, h and L. However, these four parameters are dependent on each other and it turns out we only need to specify three parameters to uniquely specify the wave. This is because a connection between the wave length and the wave period exists, i.e. the longer the wave period the longer the wave length for a given water depth. This relationship is called the *dipersion relationship* which is derived in the following.

The dispersion relationship is determined by inserting Eq. 3.36 into the linearised free surface boundary condition (Eq. 3.24), $\frac{\partial\varphi}{\partial z} + \frac{\omega^2}{g}\frac{\partial^2\varphi}{\partial\theta^2} = 0$ for $z = 0$.

$$\begin{aligned} \text{As} \quad \frac{\partial\varphi}{\partial z} &= A\,C\,k\,\frac{sinh\;,k\,(z+h)}{sinh\,kh}\,sin\theta \\ \text{and} \quad \frac{\partial^2\varphi}{\partial\theta^2} &= A\,C\,\frac{cosh\,k\,(z+h)}{sinh\,kh}\,(-sin\theta) \end{aligned}$$

We find by substitution into Eq. 3.24 and division by AC:

$$\omega^2 = g\,k\,tanh\,kh \tag{3.40}$$

which could be rewritten by inserting $\omega = \frac{2\pi}{T}$, $k = \frac{2\pi}{L}$ and $L = c \cdot T$ to get:

$$c = \sqrt{\frac{g\,L}{2\pi}\,tanh\,\frac{2\pi h}{L}} \tag{3.41}$$

This equation shows that waves with different wave length in general have different propagation velocities, i.e. the waves are dispersive. Therefore, this equation is often refered to as the *dispersion relationship*, no matter if the formulation in Eq. 3.40 or Eq. 3.41 is used. We can conclude that if h and H are given, which is the typical case, it is enough to specify only one of the parameters c, L and T. The simplest case is if h, H and L are specified (geometry specified), as we directly from Eq. 3.41 can calculate c and afterwards $T = \frac{L}{c}$. However, it is much easier to measure the wave period T than the wave length L, so the typical case is that h, H and T are given. However, this makes the problem somewhat more complicated as L cannot explicitly be determined for a given set of h, H and T. This can be see by rewriting the dispersion relation (Eq. 3.41) to the alternative formulation:

$$L = \frac{g\,T^2}{2\pi}\,tanh\,\frac{2\pi h}{L} \tag{3.42}$$

From this we see that L has to be found by iteration. In the literature it is possible to find many approximative formulae for the wave length, e.g. the formula by Hunt, 1979 or Guo, 2002. However, the iteration procedure is simple and straight forward but the approximations can be implemented as the first guess in the numerical iteration. The Guo, 2002 formula is based on logarithmic matching and reads:

$$L = \frac{2\pi h}{x^2(1 - exp(-x^{\beta}))^{-1/\beta}} \tag{3.43}$$

where $x = h\omega/\sqrt{gh}$ and $\beta = 2.4908$.

The velocity potential can be rewritten in several waves by including the dispersion relation. One version is found by including Eq. 3.40 in Eq. 3.39 to get:

$$\varphi = -a\,c\,\frac{cosh\,k(z+h)}{sinh\,kh}\,sin(\omega t - kx) \tag{3.44}$$

3.6 Particle Velocities and Accelerations

The *velocity field* can be found directly by differentiation of the velocity potential given in Eq. 3.39 or an alternatively form where the dispersion relation has been included (e.g. Eq. 3.44).

$$
\begin{aligned}
u = \frac{\partial \varphi}{\partial x} &= \frac{a\,g\,k}{\omega}\,\frac{cosh\,k(z+h)}{cosh\,kh}\,cos(\omega t - kx) \\
&= a\,c\,k\,\frac{cosh\,k(z+h)}{sinh\,kh}\,cos(\omega t - kx) \\
&= a\,\omega\,\frac{cosh\,k(z+h)}{sinh\,kh}\,cos(\omega t - kx) \\
&= \frac{\pi\,H}{T}\,\frac{cosh\,k(z+h)}{sinh\,kh}\,cos(\omega t - kx)
\end{aligned} \tag{3.45}
$$

$$
\begin{aligned}
w = \frac{\partial \varphi}{\partial z} &= -\frac{a\,g\,k}{\omega}\,\frac{sinh\,k(z+h)}{cosh\,kh}\,sin(\omega t - kx) \\
&= -a\,c\,k\,\frac{sinh\,k(z+h)}{sinh\,kh}\,sin(\omega t - kx) \\
&= -a\,\omega\,\frac{sinh\,k(z+h)}{sinh\,kh}\,sin(\omega t - kx) \\
&= -\frac{\pi\,H}{T}\,\frac{sinh\,k(z+h)}{sinh\,kh}\,sin(\omega t - kx)
\end{aligned} \tag{3.46}
$$

The *acceleratation field* for the particles is found by differentiation of Eqs. 3.45 and 3.46 with respect to time. It turns out that for the linear theory the total accelerations can be approximated by the local acceleration as the convective part are of higher order.

$$
\frac{du}{dt} \approx \frac{\partial u}{\partial t} = -a\,g\,k\,\frac{cosh\,k(z+h)}{cosh\,kh}\,sin(\omega t - kx) \tag{3.47}
$$

$$
\frac{dw}{dt} \approx \frac{\partial w}{\partial t} = -a\,g\,k\,\frac{sinh\,k(z+h)}{cosh\,kh}\,cos(\omega t - kx) \tag{3.48}
$$

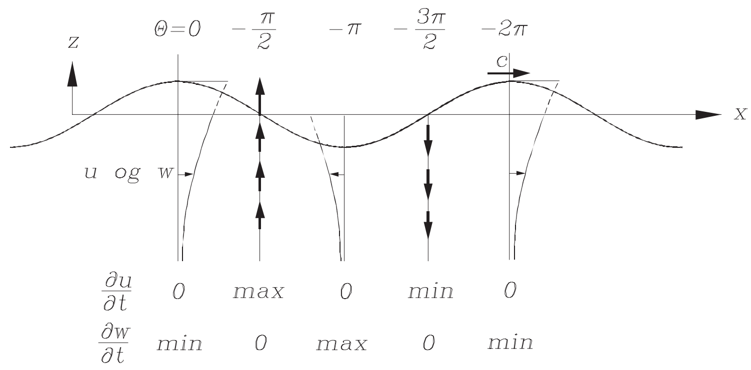

Theoretically the expressions in Eqs. 3.46 to 3.48 is only valid for $\frac{H}{L} << 1$, i.e. in the interval $-h < z \simeq 0$. However, it is quite common practise to use the expressions for finite positive and negative values of η, i.e. also for $z = \eta$. However, this can only give a very crude approximation as the theory breaks down near the surface. Alternatively the so-called Wheeler stretching of the velocity and acceleration profiles can be applied, where the profiles are stretched and compressed so that the evaluation coordinate (z_c) is never positive. The evaluation coordinate is given by $z_c = \frac{h(z-\eta)}{h+\eta}$ where η is the instantaneous water surface elevation. This type of stretching is commonly used for irregular linear waves where the velocity of each component is stretched to the real surface, i.e. the sum of all η components.

3.7 Pressure Field

The pressure variations are calculated from the Bernoulli equation, Eq. 2.4:

$$gz + \frac{p}{\rho} + \frac{1}{2}\left(\left(\frac{\partial \varphi}{\partial x}\right)^2 + \left(\frac{\partial \varphi}{\partial z}\right)^2\right) + \frac{\partial \varphi}{\partial t} = 0 \tag{3.49}$$

The reference pressure for $z = 0$, i.e. the atmospheric pressure is here set equal to zero. As a consequence the pressure p is the excess pressure relative to the atmospheric pressure. The quadratic terms are small when $H/L << 1$ as shown earlier in the linearisation of the dynamic surface boundary condition. The linearised Bernoulli equation reads:

$$gz + \frac{p}{\rho} + \frac{\partial \varphi}{\partial t} = 0 \tag{3.50}$$

We now define the dynamic pressure p_d which is the wave induced pressure, i.e. the excess pressure relative to the hydrostatic pressure (and the atmospheric pressure), i.e.:

$$p_d \equiv p - \rho g(-z) = p + \rho\, g\, z \tag{3.51}$$

which when inserted into Eq. 3.50 leads to:

$$p_d = -\rho \frac{\partial \varphi}{\partial t} \tag{3.52}$$

From Eq. 3.51 we get:

$$p_d = \rho\, g\, \frac{H}{2} \frac{\cosh k(z+h)}{\cosh kh} \cos(\omega t - kx) \tag{3.53}$$

As $\eta = \frac{H}{2} \cos(\omega t - kx)$, we can also write Eq. 3.53 as:

$$p_d = \rho\, g\, \eta \frac{\cosh k(z+h)}{\cosh kh}\ , \text{ which at } z = 0 \text{ gives } \ p_d = \rho\, g\, \eta \tag{3.54}$$

This means the pressure is in phase with the surface elevation and with decreasing amplitude towards the bottom. The figure below shows the pressure variation under the wave crest.

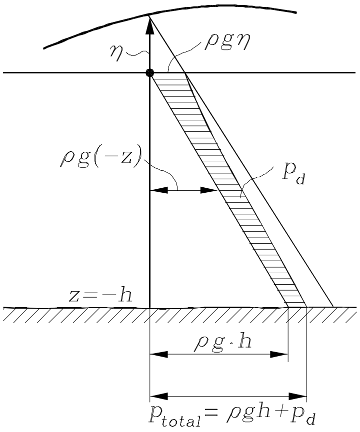

For $z > 0$, where the previous derivations are not valid, we can make a crude approximation and use hydrostatic pressure distribution from the surface, i.e. $p_{total} = \rho g(\eta - z)$ giving $p_d = \rho g\eta$.

Wave height estimations from pressure measurements

Waves in the laboratory and in the prototype can be measured in several ways. The most common in the laboratory is to measure the surface elevation directly by using resistance or capacitance type electrical wave gauges. However, in the prototype this is for practical reasons seldom used unless there is already an existing structure where you can mount the gauge. In the prototype it is more common to use buoys or pressure transducers, which both give rise to some uncertainties. For the pressure transducer you assume that the waves are linear so you can use the linear transfer function from pressure to surface elevations. For a regular wave this is easy as you can use:

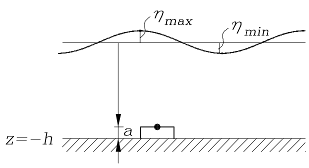

Highest measured pressure (p_{max}):

$$\rho\, g(h-a) + \rho\, g\, \eta_{max} \frac{\cosh k(-(h-a)+h)}{\cosh kh}$$

Lowest measured pressure (p_{min}):

$$\rho\, g(h-a) + \rho\, g\, \eta_{min} \frac{\cosh k(-(h-a)+h)}{\cosh kh}$$

$$p_{max} - p_{min} = \rho g \frac{\cosh ka}{\cosh kh} \cdot (\eta_{max} - \eta_{min})$$

In case of irregular waves you cannot use the above give procedure as you have a mix of frequencies. In that case you have to split the signal into the different frequencies, cf. section 5.3. The position of the pressure transducer is important as you need to locate it some distance below the lowest surface elevation you expect. Moreover, you need a significant variation in the pressure compared to the noise level for the frequencies considered important. This means that if you have deep water waves you cannot put the pressure gauge close to the bottom as the wave induced pressures will be extremely small.

3.8 Linear Deep and Shallow Water Waves

In the literature the terms deep and shallow water waves can be found. These terms corresponds to the water depth is respectively large and small compared to the wave length. It turns out the linear equations can be simplified in these cases. The two cases will be discussed in the following sections and the equations will be given.

3.8.1 Deep Water Waves

When the water depth becomes large compared to the wave length $kh = \frac{2\pi h}{L} \rightarrow \infty$, the wave is no longer influence by the presence of a bottom and hence the water depth h must vanish from the equations. Therefore, the expressions describing the wave motion can be simplified compared to the general case. The equations are strictly speaking only valid when kh is infinite, but it turns out that these simplified equations are excellent approximations when $kh > \pi$ corresponding to $\frac{h}{L} > \frac{1}{2}$.

Commonly indice 0 is used for deep water waves, i.e. L_0 is the deep water wave length. From Eq. 3.42 we find:

$$L_0 = \frac{g\,T^2}{2\pi} \quad \text{or} \quad T = \sqrt{\frac{2\pi}{g}\,L_0} \quad \text{or} \quad c_0 = \sqrt{\frac{g}{k_0}} \tag{3.55}$$

as $tanh(kh) \rightarrow 1$ for $kh \rightarrow \infty$. Therefore, we can conclude that in case of deep water waves the wave length only depends on the wave period as the waves doesn't feel the bottom. Note that there is no index on T, as this does not vary with the water depth.

From Appendix A we find $cosh\,\alpha$ and $sinh\,\alpha \rightarrow \frac{1}{2}\,e^{\alpha}$ for $\alpha \rightarrow \infty$ and $tanh\,\alpha$ and $coth\,\alpha \rightarrow 1$ for $\alpha \rightarrow \infty$. Therefore, we find the following deep water expressions from Eqs. 3.44, 3.45, 3.46 and 3.53:

$$\begin{aligned} \varphi &= -\frac{H_0\,L_0}{2\,T}\,e^{k_0 z} sin(\omega t - k_0 x) \\ u &= \frac{\pi\,H_0}{T}\,e^{k_0 z}\,cos(\omega t - k_0 x) \\ w &= -\frac{\pi\,H_0}{T}\,e^{k_0 z}\,sin(\omega t - k_0 x) \\ p_d &= \rho g\,\frac{H_0}{2}\,e^{k_0 z}\,cos(\omega t - k_0\,x) \end{aligned} \tag{3.56}$$

Even though these expressions are derived for $kh \rightarrow \infty$ they are very good approximations for $h/L > \frac{1}{2}$.

3.8.2 Shallow Water Waves

For shallow water waves, i.e. $kh \to 0$, we can also find simplified expressions. As $tanh\,\alpha \to \alpha$ for $\alpha \to 0$ we find from Eq. 3.41 or 3.42:

$$L = \frac{g\,T^2\,h}{L} \quad , \quad T = \sqrt{\frac{L^2}{g\,h}} \quad , \quad L = T\sqrt{g\,h} \;\; , \;\; c = \sqrt{g\,h} \tag{3.57}$$

From which we can conclude that the phase velocity c depends only of the water depth, and in contrast to the deep water case is thus independent of the wave period. Shallow water waves are thus non-dispersive, as all components propagate with the same velocity.

As $cosh\,\alpha \to 1$, $sinh\,\alpha \to \alpha$ and $tanh\alpha \to \alpha$ for $\alpha \to 0$ we find:

$$\begin{aligned}
\varphi &= -\frac{H\,L}{2\,T}\frac{1}{k\,h}\,sin(\omega t - kx) \\
u &= \frac{H}{2}\frac{L}{Th}\,cos(\omega t - kx) \\
w &= -\frac{\pi\,H}{T}\,\frac{z+h}{h}\,sin(\omega t - kx) \\
p_d &= \rho\,g\,\frac{H}{2}\,\frac{z+h}{h}\,cos(\omega t - kx)
\end{aligned}$$

These equations are good approximations for $h/L < \frac{1}{20}$.

3.9 Particle Paths

The previously derived formulae for the particle velocities (Eqs. 3.45 and 3.46) describe the velocity field with respect to a fixed coordinate, i.e. an Eulerian description. In this section we will describe the particle paths $(x(t), z(t))$, i.e. a Lagrange description. In general the particle paths can be determined by integrating the velocity of the particle in time, which means solving the following two equations:

$$\frac{dx}{dt} = u(x, z, t) \qquad \frac{dz}{dt} = w(x, z, t) \tag{3.58}$$

where the particle velocity components u and w are given by Eqs. 3.45 and 3.46. These equations (3.58) cannot be solved analytically because of the way u and w depend on x and z.

We utilize the small amplitude assumption, $H/L << 1$, to linearize Eq. 3.58. Based on the expressions of u, w and visual observations we assume the particle paths are closed orbits and we can introduce a mean particle position $(x, z) = (\xi, \zeta)$. Moreover, based on the 1. order theory we assume that, the particle oscillations $\Delta x, \Delta z$ from respectively ξ and ζ are small compared to the wave length, L, and water depth, h. We can write the instantaneous particle position (x, z) as:

$$x = \xi + \Delta x \qquad \text{and} \qquad z = \zeta + \Delta z \tag{3.59}$$

We now insert Eq. 3.59 into Eqs. 3.45 and 3.46, and make a Taylor expansion of the sin, cos, sinh and cosh functions from the mean position (ξ, ζ). Terms of higher order are discarded and here after we can solve Eq. 3.58 with respect to x and z.

By using the taylor series expansion:

$$f(a + \Delta a) = f(a) + \frac{f'(a)}{1!}\,\Delta a + \frac{f''(a)}{2!}\,\Delta a^2 + \dots$$

we get by introducing Eq. 3.59 the following series expansions of sinh, cosh, sin and cos.

$$\begin{aligned}
sinh\,k(z+h) &= sinh\,k(\zeta+h) + k\,cosh\,k(\zeta+h)\cdot\Delta z + \dots \\
cosh\,k(z+h) &= cosh\,k(\zeta+h) + k\,sinh\,k(\zeta+h)\cdot\Delta z + \dots \\
sin(\omega t - kx) &= sin(\omega t - k\xi) + (-k)cos(\omega t - k\xi)\cdot\Delta x + \dots \\
cos(\omega t - kx) &= cos(\omega t - k\xi) - (-k)sin(\omega t - k\xi)\cdot\Delta x + \dots
\end{aligned} \tag{3.60}$$

If we insert Eqs. 3.45 and 3.58 we get for the x-coordinate:

$$\begin{aligned}
\frac{dx}{dt} \simeq\; & \frac{\pi H}{T}\,\frac{cosh\,k(\zeta+h) + k\,\Delta\,z\,sinh\,k(\zeta+h)}{sinh\,kh}\,(cos(\omega t - k\xi) \\
& + k\,\Delta\,x\,sin(\omega t - k\xi))
\end{aligned}$$

As $k\Delta z$ and $k\Delta x = \sigma\left(\frac{H}{L}\right) << 1$ we find the linearised expression:

$$\frac{dx}{dt} \simeq \frac{\pi H}{T}\,\frac{cosh\,k(\zeta+h)}{sinh\,kh}\,cos(\omega t - k\xi) \tag{3.61}$$

and equivalent for dz/dt:

$$\frac{dz}{dt} \simeq -\frac{\pi H}{T}\,\frac{sinh\,k(\zeta+h)}{sinh\,kh}\,sin(\omega t - k\xi) \tag{3.62}$$

By integration we find:

$$x = \frac{\pi H}{T\omega}\,\frac{cosh\,k(\zeta+h)}{sinh\,kh}\,sin(\omega t - k\xi) + C \tag{3.63}$$

This equation could also be written as:

$x = \mathcal{K}\,sin(\omega t - k\xi) + C$ or $\mathcal{K}\,sin\theta + C$, where θ has the cycle 2π.

The mean position $\xi \equiv \overline{x} = \dfrac{1}{2\pi}\displaystyle\int_0^{2\pi} \mathcal{K}\, sin\theta\, d\theta + C = 0 + C,$ hence $C = \xi.$

$$\begin{aligned} x &= \xi + \frac{H}{2}\,\frac{cosh\,k(\zeta+h)}{sinh\,kh}\,sin(\omega t - k\xi) \\ &\text{and by equivalent calculations we get:} \\ z &= \zeta + \frac{H}{2}\,\frac{sinh\,k(\zeta+h)}{sinh\,kh}\,cos(\omega t - k\xi) \end{aligned} \tag{3.64}$$

Eq. 3.64 could be written as:

$$\begin{aligned} x - \xi &= A(\zeta) sin\theta \\ z - \zeta &= B(\zeta) cos\theta \end{aligned}$$

By squaring and summation we get, as $\sqrt{cos^2\theta + sin^2\theta} = 1$:

$$\left(\frac{x-\xi}{A(\zeta)}\right)^2 + \left(\frac{z-\zeta}{B(\zeta)}\right)^2 = 1 \quad ,$$

Leading to the conclusion that the particle paths are for linear waves elliptical with center (ξ, ζ) and $A(\zeta)$ and $B(\zeta)$ are horizontal and vertical amplitude respectively. Generally speaking the amplitudes are a function of ζ, i.e. the depth. At the surface the vertical amplitude is equal to $H/2$ and the horizontal one is equal to $H/2\, coth\, kh$. Below is a figure showing the particle paths, the foci points and the amplitudes.

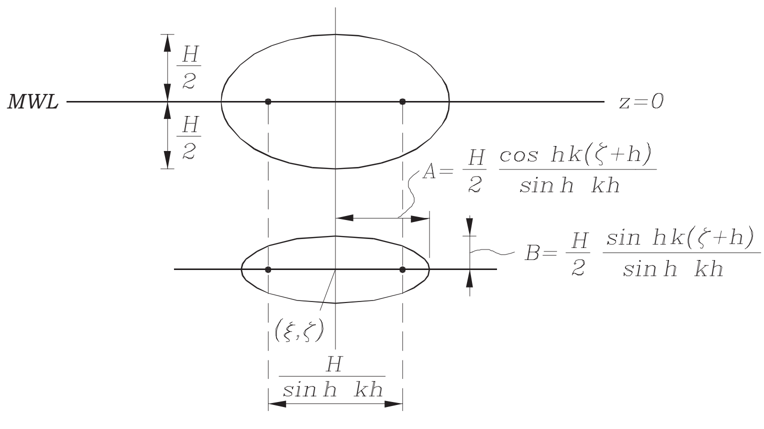

3.9.1 Deep Water Waves

We will now consider the deep water case $\frac{h}{L} > \frac{1}{2}$, corresponding to $kh = \frac{2\pi h}{L} > \pi$ we have $cosh\, kh \simeq \frac{1}{2}\, e^{kh}$ and $sinh\, kh \simeq \frac{1}{2}\, e^{kh}$.

By using $\frac{cosh\, k(\zeta+h)}{sinh\, kh} = \frac{coshk\zeta\, cosh\, kh + sinh\, k\zeta \cdot sinh\, kh}{sinh\, kh}$ we find:

$$A(\zeta) \simeq \frac{H}{2} e^{k\zeta}$$

$$B(\zeta) \simeq \frac{H}{2} e^{k\zeta}$$

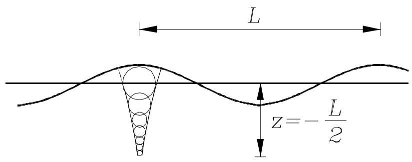

Leading to the conclusion that when we have deep water waves, the particle paths are circular with radius $A = B$. At the surface the diameter is naturally equal to the wave height H. At the depth $z = -\frac{L}{2}$ the diameter is only approx. 4% of H. We can thus conclude that the wave do not penetrate deep into the ocean.

3.9.2 Shallow Water Waves

For the shallow water case $\frac{h}{L} < \frac{1}{20}$, corresponding to $kh = \frac{2\pi h}{L} < \frac{\pi}{10}$ we find, as $cosh\, kh \simeq 1$ and $sinh\, kh \simeq kh$:

$$\begin{aligned} A(\zeta) &\simeq \frac{H}{2}\frac{1}{kh} && \text{, i.e. constant over depth} \\ B(\zeta) &\simeq \frac{H}{2}(1+\frac{\zeta}{h}) && \text{, i.e. linearly decreasing with depth.} \end{aligned}$$

3.9.3 Summary and Discussions

Below are the particle paths illustrated for three different water depths.

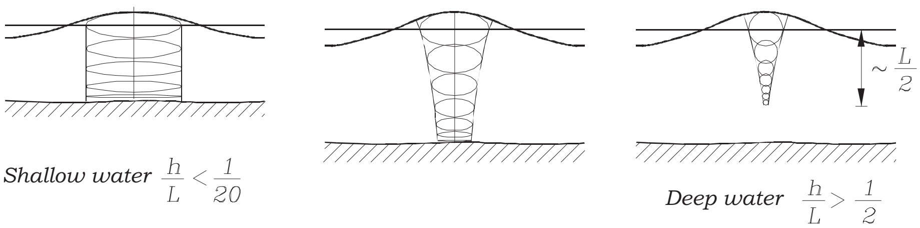

The shown particle paths are for small amplitude waves. In case of finite amplitude waves the particle paths are no longer closed orbits and a net transport of water can be observed. This is because the particle velocity in the upper part of the orbit is larger than in the lower part of the orbit.

When small wave steepness the paths are closed orbits (general ellipses):

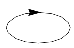

When large wave steepness the paths are open orbits, i.e. net mass transport:

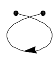

However, the transport velocity is even for steep waves smaller than 4% of the phase speed c. Below is the velocity vectors and particle paths drawn for one wave period.

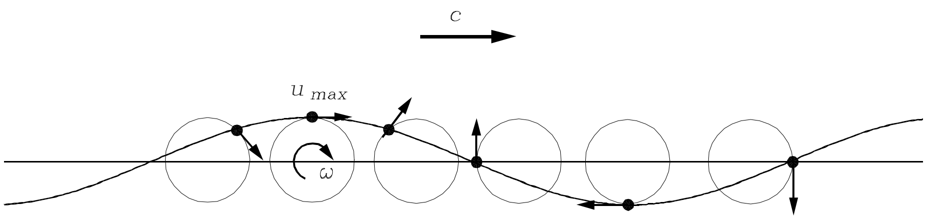

$u_{max} < c$ for deep water waves. For $H/L = 1/7$ we find $u_{max} \simeq 0,45c$

3.10 Wave Energy and Energy Transportation

When we talk of wave energy we normally think of the mechanical energy content, i.e. kinetic and potential energy. The kinetic energy originates from the movement of the particles and the potential energy originates from the displacement of the water surface from a horizontal plane surface.

The amount of heat energy contained in the fluid is of no interest as the heat energy never can be converted to mechanical wave energy again. However, the transformation of mechanical energy to heat energy is interesting, as it describes the 'loss' of mechanical energy. Wave breaking is in most cases the main contributor to the loss in mechanical energy. In the description of certain phenomena, such as for example wave breaking, it is important to know the amount of energy that is transformed.

The energy in the wave can be shown to propagate in the wave propagation direction. In fact the wave propagation direction is defined as the direction the energy propagate.

3.10.1 Kinetic Energy

As we consider an ideal fluid there is no turbulent kinetic energy present. Therefore, we only consider the particle velocities caused by the wave itself. The instantaneous kinetic energy per unit volume $e_k(\theta)$ is:

$$\begin{aligned} e_k(\theta) &= \frac{1}{2}\rho(u^2 + w^2) \\ e_k(\theta) &= \frac{1}{2}\rho(\frac{H\omega}{2sinhkh})^2[cosh^2k(z+h)cos^2\theta + sinh^2k(z+h)sin^2\theta)] \\ e_k(\theta) &= \frac{1}{4}\rho\frac{gkH^2}{sinh2kh}[cos^2\theta + sinh^2k(z+h)] \end{aligned} \tag{3.65}$$

The instantaneous kinetic energy per unit area in the horizontal plane $E_k(\theta)$ is found by integrating $e_k(\theta)$ from the bottom ($z = -h$) to the surface ($z = \eta$). However, as it mathematically is very complicated to integrate to the surface, is instead chosen to do the integration to the mean water level ($z = 0$). It can easily be shown that the error related to this is small when $H/L << 1$.

$$E_k(\theta) \;=\; \frac{1}{4}\rho\frac{gkH^2}{sinh2kh}\left(h\,cos^2\theta + \frac{1}{2}\int_{-h}^{0}\left[cosh2k(z+h) - 1\right]dz\right)$$

where $sinh^2(x) = \frac{e^{2x}+e^{-2x}-2}{4} = \frac{1}{2}[cosh(2x)-1]$ has been used. After performing the integration and rearranging we get:

$$E_k(\theta) \;=\; \frac{1}{16}\rho g H^2 + \frac{1}{8}\rho g H^2 \frac{2kh}{sinh2kh}\left[cos^2\theta - \frac{1}{2}\right] \tag{3.66}$$

If we average over one wave period T or one wave length L (which gives identical results for waves with constant form), we get the mean value of the kinetic energy E_k to:

$$E_k = \frac{1}{16}\rho g H^2 \tag{3.67}$$

as the mean value of $cos^2(\theta)$ over one period is 1/2.

3.10.2 Potential Energy

As the fluid is assumed incompressible and surface tension is neglected all the potential energy originates from the gravitational forces. Further, we deal only with the energy caused by displacement of the water surface from the mean water level. With these assumptions we can write the instantaneous value of the potential energy $E_p(\theta)$ per unit area in the horizontal plane as:

$$\begin{aligned}
E_p(\theta) &= \int_{-h}^{\eta} \rho g z dz - \int_{-h}^{0} \rho g z dz \\
E_p(\theta) &= \int_{0}^{\eta} \rho g z dz \\
E_p(\theta) &= \frac{1}{2}\rho g \eta^2 \qquad (3.68)
\end{aligned}$$

Averaging over one wave period T or one wave length L gives the mean value of the potential energy E_p:

$$\begin{aligned}
E_p &= \frac{1}{2}\rho g \overline{\eta^2} \\
E_p &= \frac{1}{2}\rho g \frac{H^2}{4}\overline{cos^2\theta} \quad \text{(for linear waves)} \\
E_p &= \frac{1}{16}\rho g H^2 \qquad (3.69)
\end{aligned}$$

3.10.3 Total Energy Density

The total wave energy density per unit area in the horizontal plane E is the sum of the kinetic energy density E_k and the potential energy density E_p.

$$E = E_k + E_p$$
$$E = \frac{1}{8}\rho g H^2 \qquad (3.70)$$

3.10.4 Energy Flux

As the waves travel across the ocean they carry their potential an kinetic energy with them. However, the energy density in the waves can not directly be related to an energy equation for the wave motion. In that case we need to consider the average energy (over one period) that is transported through a fixed vertical section and integrated over the depth. If this section is parallel to the wave fronts and has a width of 1 m, it is called the mean transported energy flux or simply the energy flux E_f.

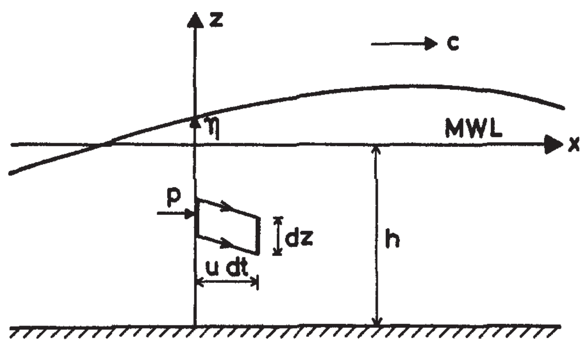

Figure 3.1: Definitions for calculating energy flux.

We now consider the element shown in Fig. 3.1. The energy flux through the shown vertical section consist partly of the transported mechanical energy contained in the control volume, and partly of the increase in kinetic energy, i.e. the work done by the external forces.

Work produced by external forces:
On a vertical element dz acts the horizontal pressure force pdz. During the time interval dt the element moves the distance udt to the right. The work produced per unit width A (force x distance) is thus:

$$A = \Delta E_k = p\ u\ dz\ dt$$

Mechanical energy:
The transported mechanical energy through the vertical element dz per unit width is calculated as:

$$E_{f,mec} = [\rho g z + \frac{1}{2}\rho(u^2 + w^2)]u \; dz \; dt$$

Energy flux:
The instantaneous energy flux $E_f(t)$ per unit width is:

$$E_f(t) = \int_{-h}^{\eta} [p + \rho g z + \frac{1}{2}\rho(u^2 + w^2)] u dz$$

After neglecting the last term which is of higher order, change of upper integration limit to $z = 0$, and introduction of the dynamic pressure $p_d = p + \rho g z$ we get:

$$E_f(t) = \int_{-h}^{0} p_d \, u \, dz \qquad (3.71)$$

Note that the symbol p^+ (excess pressure) can be found in some literature instead of p_d.

The mean energy flux E_f (often just called the energy flux) is calculated by integrating the expression 3.71 over one wave period T, and insertion of the expressions for p_d and u.

$$E_f = \overline{E}_f(t)$$

$$E_f = \frac{1}{16}\rho g H^2 c[1 + \frac{2kh}{sinh 2kh}] \qquad (3.72)$$

$$E_f = E c_g \qquad (3.73)$$

where we have introduced the energy propagation velocity $c_g = c(\frac{1}{2} + \frac{kh}{sinh2kh})$. The energy propagation velocity is often called the group velocity as it is related to the velocity of the wave groups, cf. section 3.10.5

If we take a look at the distribution of the transported energy over the depth we will observe that for deep water waves (high kh) most of the energy is close to the free surface. For decreasing water depths the energy becomes more and more evenly distributed over the depth. This is illustrated in Fig. 3.2.

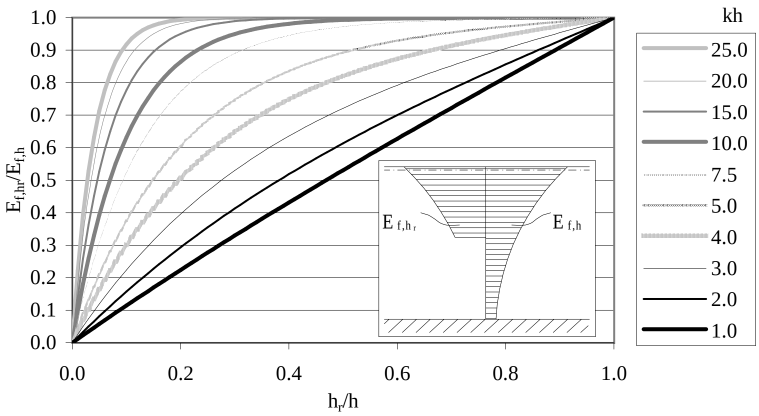

Figure 3.2: Distribution of the transported energy over the water depth.

3.10.5 Energy Propagation and Group Velocity

The energy in the waves travels as mentioned above with the velocity c_g. However, c_g also describes the velocity of the wave groups (wave packets), which is a series of waves with varying amplitude. As a consequence c_g is often called the group velocity. In other words the group velocity is the speed of the envelope of the surface elevations.

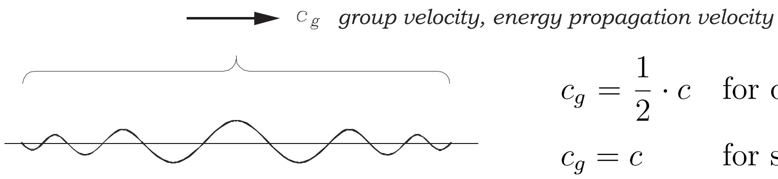

$$c_g = \frac{1}{2} \cdot c \quad \text{for deep water waves}$$

$$c_g = c \quad \text{for shallow water waves}$$

This phenomena can easy be illustrated by summing two linear regular waves with slightly different frequencies, but identical amplitudes and direction. These two components travel with different speeds, cf. the dispersion relationship. Therefore, they will reinforce each other at one moment but cancel out in another moment. This will repeat itself over and over again, and we get an infinite number of wave groups formed.

Another way to observe wave groups is to observe a stone dropped into water to generate some few deep water waves.

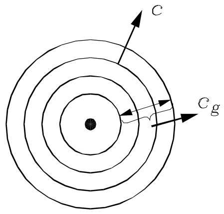

Stone drop in water generates ripples of circular waves, where the individual wave overtake the group and disappear at the front of the group while new waves develop at the tail of the group.

One important effect of deep water waves being dispersive (c and c_g depends on the frequency) is that a field of wind generated waves that normally consist of a spectrum of frequencies, will slowly separate into a sequence of wave fields, as longer waves travel faster than the shorter waves. Thus when the waves after traveling a very long distance hit the coast the longer waves arrive first and then the frequency slowly increases with time. The waves generated in such a way are called swell waves and are very regular and very two-dimensional (long-crested).

In very shallow water the group velocity is identical to the phase velocity, so the individual waves travel as fast as the group. Therefore, shallow water waves maintain there position in the wave group.

3.11 Evaluation of Linear Wave Theory

In the previous pages is the simplest mathematical model of waves derived and described. It is obvious for everyone, who has been at the coast, that real waves are not regular monochromatic waves (sine-shaped). Thus the question that probably arise is: When and with what accuracy can we use the linear theory for regular waves to describe real waves and their impact on ships, coasts, structures etc.?

The developed theory is based on regular and linear waves. In engineering practise the linear theory is used in many cases. However, then it is in most cases irregular linear waves that are used. Irregular waves is the topic of Chapter 5. In case regular waves are used for design purposes it is most often a non-linear theory that is used as the Stokes 5. order theory or the stream function theory. Waves with finite height (non-linear waves) is outside the scope of this short note, but will be introduced in the next semester.

To distinguish between linear and non-linear waves we classify the waves after their steepness:

$H/L \to 0$, waves with small amplitude 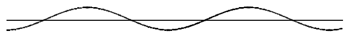
1. order Stokes waves, linear waves, Airy waves, monochromatic waves.

$H/L > 0.01$, waves with finite height 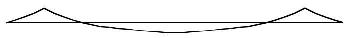
higher order waves, e.g. 5. order Stokes waves.

Even though the described linear theory has some shortcomings, it is important to realise that we already (after two lectures) are able to describe waves in a sensible way. It is actually impressive the amount of problems that can be solved by the linear theory. However, it is also important to be aware of the limitations of the linear theory.

From a physically point of view the difference between the linear theory and higher order theories is, that the higher order theories take into account the influence of the wave itself on its characteristics. Therefore, the shape of the surface, the wave length and the phase velocity all becomes dependent on the wave height.

Linear wave theory predicts that the wave crests and troughs are of the same size. Theories for waves with finite height predicts the crests to significant greater than the troughs. For high steepness waves the trough is only around 30 percent of the wave height. This is very important to consider for design of e.g. top-sites for offshore structure (selection of necessary level). The use of the linear theory will in such cases lead to very unsafe designs. This shows that it is important to understand the differences between the theories and their validity.

Linear wave theory predicts the particle paths to be closed orbits. Theories for waves with finite height predicts open orbits and a net mass flow in the direction of the wave.

Chapter 4

Changes in Wave Form in Coastal Waters

Most people have noticed that the waves changes when they approach the coast. The change affect both the height, length and direction of the waves. In calm weather with only small swells these changes are best observed. In such a situation the wave motion far away from the coast will be very limited. If the surface elevation is measured we would find that they were very close to small amplitude linear waves, i.e. sine shaped. Closer to the coast the waves becomes affected by the limited water depth and the waves raises and both the wave height and especially the wave steepness increases. This phenomena is called shoaling. Closer to the coast when the wave steepness or wave height has become too large the wave breaks.

The raise of the waves is in principle caused by three things. First of all the decreasing water depth will decrease the wave propagation velocity, which will lead to a decrease in the wave length and thus the wave steepness increase. Second of all the wave height increases when the propagation velocity decreases, as the energy transport should be the same and as the group velocity decreases the wave height must increase. Finally, does the increased steepness result in a more non-linear wave form and thus makes the impression of the raised wave even more pronounced.

The change in the wave form is solely a result of the boundary condition that the bottom is a streamline. Theoretical calculations using potential theory gives wave breaking positions that can be reproduced in the laboratory. Therefore, the explanation that wave breaking is due to friction at the bottom must be wrong.

Another obvious observation is that the waves always propagate towards the coast. However, we probably all have the feeling that the waves typically propagate in the direction of the wind. Therefore, the presence of the coast must affect the direction of the waves. This phenomenon is called wave refraction and is due to the wave propagation velocity depends on the water depth.

These depth induced variations in the wave characteristics (height and direction) are usually sufficiently slow so we locally can apply the linear theory for waves on a horizontal bottom. When the non-linear effects are too strong we have to use a more advanced model for example a Boussinesq model.

In the following these shallow water phenomena are discussed. An excellent location to study these phenomena is Skagens Gren (the northern point of Jutland).

4.1 Shoaling

We investigate a 2-dimensional problem with parallel depth contours and where the waves propagate perpendicular to the coast (no refraction). Moreover, we assume:

- Water depth vary so slowly that the bottom slope is everywhere so small that there is no reflection of energy and so we locally can apply the linear theory for progressive waves with the horizontal bottom boundary condition. The relative change in water depth over one wave length should thus be small.
- No energy is propagating across wave orthogonals, i.e. the energy is propagating perpendicular to the coast (in fact it is enough to assume the energy exchange to be constant). This means there must be no current and the waves must be long-crested.
- No wave breaking.
- The wave period T is unchanged and hence f and ω are also unchanged. This seems valid when there is no current and the bottom has a gentle slope.

The energy content in a wave per unit area in the horizontal plane is:

$$E = \frac{1}{8}\rho g H^2 \tag{4.1}$$

The energy flux through a vertical section is E multiplied by the energy propagation velocity c_g:

$$P = Ec_g \tag{4.2}$$

Inserting the expressions from Eq. 3.73 gives:

$$P = \frac{1}{8}\rho g H^2 \cdot c\,(\frac{1}{2} + \frac{kh}{sinh(2kh)}) \tag{4.3}$$

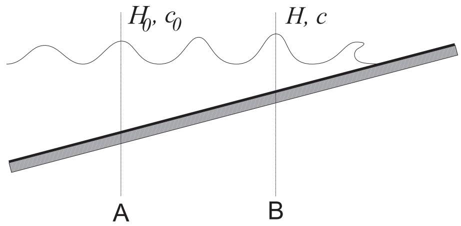

Figure 4.1: Definitions for calculating 2-dimensional shoaling (section A is assumed to be on deep water).

Due to the assumptions made the energy is conserved in the control volume. Thus the energy amount that enters the domain must be identical to the energy amount leaving the domain. Moreover, as we have no energy exchange perpendicular to the wave orthogonals we can write:

$$E^A \cdot {c_g}^A = E^B \cdot {c_g}^B \tag{4.4}$$

$$H^B = H^A \sqrt{\frac{{c_g}^A}{{c_g}^B}} \tag{4.5}$$

The above equation can be used between two arbitary vertical sections, but remember the assumption of energy conservation (no wave breaking) and small bottom slopes. In many cases it is assumed that section A is on deep water and we get the following equation:

$$\frac{H}{H_0} = K_s = \sqrt{\frac{c_{0,g}}{c_g}} \tag{4.6}$$

The coefficient K_s is called the shoaling coefficient. As shown in Figure 4.1 the shoaling coefficient first drops slightly below one, when the wave approach shallower waters. However, hereafter the coefficient increase dramatically.

All in all it can thus be concluded that the wave height increases as the wave approach the coast. This increase is due to a reduction in the group velocity when the wave approach shallow waters. In fact using the linear theory we can calculate that the group velocity approaches zero at the water line, but then we have really been pushing the theory outside its range of validity.

As the wave length at the same time decreases the wave steepness grows and grows until the wave becomes unstable and breaks.

4.2 Refraction

A consequence of the phase velocity of the waves is decreasing with decreasing water depth (wave length decreases), is that waves propagating at an angle

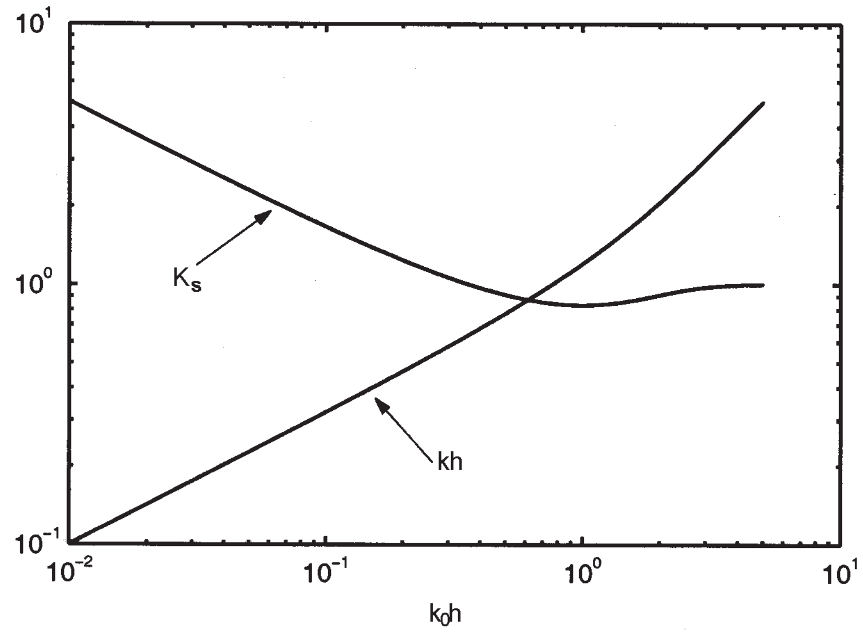

Figure 4.2: Variation of the shoaling coefficient K_s and the dimensionless depth parameter kh, as function of k_0h, where $k_0 = 2\pi/L_0$ is the deep water wave number.

(oblique incidence) toward a coast slowly change direction so the waves at last propagate almost perpendicular to the coast.

Generally the phase velocity of a wave will vary along the wave crest due to variations in the water depths. The crest will move faster in deep water than in more shallow water. A result of this is that the wave will turn towards the region with more shallow water and the wave crests will become more and more parallel to the bottom contours.

Therefore, the wave orthogonals will not be straight lines but curved. The result is that the wave orthogonals could either diverge or converge towards each other depending on the local bottom contours. In case of parallel bottom contours the distance between the wave orthogonals will increase towards the coast meaning that the energy is spread over a longer crest.

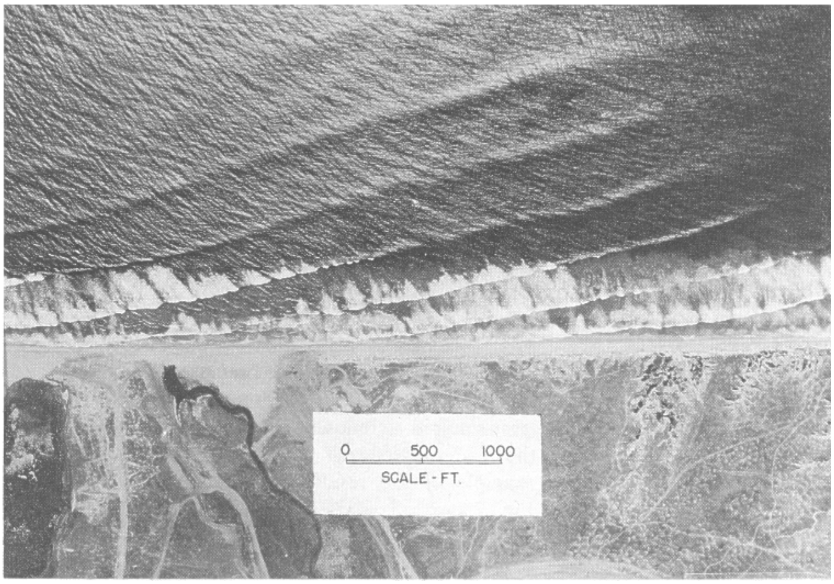

Figure 4.3: Photo showing wave refraction. The waves change direction when they approach the coast.

We will now study a case where oblique waves approach a coast. Moreover, we will just as for shoaling assume:

- Water depth vary so slowly that the bottom slope is everywhere so small that there is no reflection of energy and so we locally can apply the linear theory for progressive waves with the horizontal bottom boundary condition. The relative change in water depth over one wave length should thus be small.
- No energy is propagating across wave orthogonals, i.e. the energy is propagating perpendicular to the coast (in fact it is enough to assume the energy exchange to be constant). This means there must be no current and the waves must be long-crested.
- No wave breaking.
- The wave period T is unchanged and hence f and ω are also unchanged. This seems valid when there is no current and the bottom has a gentle slope.

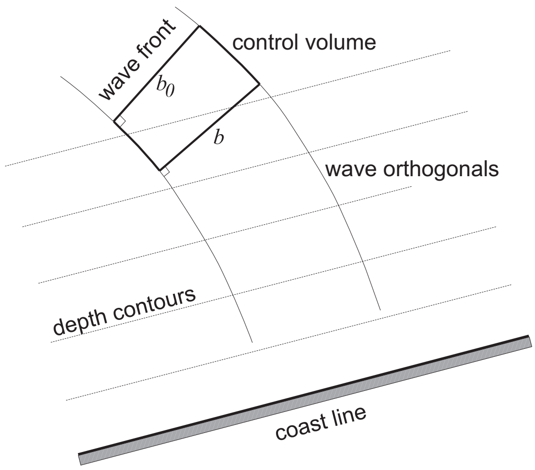

Figure 4.4: Refraction of regular waves in case of parallel bottom contours.

The energy flux P_{b_0}, passing section b_0 will due to energy conservation be identical to the energy flux P_b passing section b, cf. Fig. 4.4. The change in wave height due to changing water depth and length of the crest, can be calculated by require energy conservation for the control volume shown in Fig. 4.4:

$$E^{b_0} \cdot {c_g}^{b_0} \cdot b_0 = E^b \cdot {c_g}^b \cdot b \Rightarrow \tag{4.7}$$

$$H^b = H^{b_0} \sqrt{\frac{{c_g}^{b_0}}{{c_g}^b}} \cdot \sqrt{\frac{b_0}{b}} \Rightarrow \tag{4.8}$$

$$H^b = H^{b_0} \cdot K_s \cdot K_r \tag{4.9}$$

$$where, \quad c_g = c \cdot (\frac{1}{2} + \frac{kh}{sinh(2kh)})$$

K_r is called the refraction coefficient. In case of parallel depth contours as shown in Fig. 4.4 the refraction coefficient is smaller than unity as the length of the crests increases as the wave turns.

In the following we will shortly go through a method to calculate the refraction coefficient. The method starts by considering a wave front on deep water and then step towards the coast for a given bottom topography. The calcultion is performed by following the wave crest by stepping in time intervals Δt, e.g. 50 seconds. In each time interval is calculated the phase velocity "in each end" of the selected wave front. As the water depths in each of the ends are different the phase velocities are also different. It is now calculated the distance that each end of the wave front has tralled during the time interval Δt. Hereafter we can draw the wave front Δt seconds later. This procedure is continued until the wave front is at the coast line. It is obvious that the above given procedure requires some calculation and should be solved numerically.

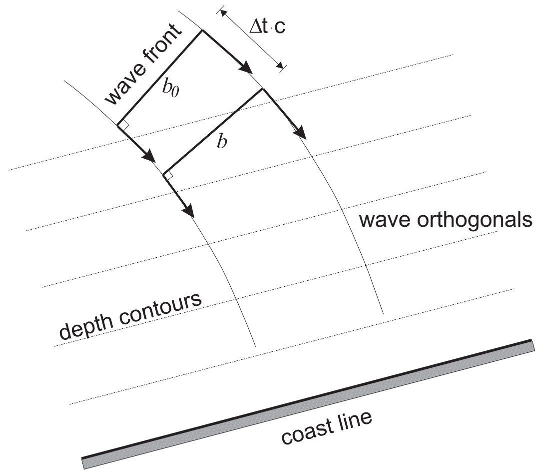

Figure 4.5: Refraction calculation.

As the wave fronts turns it must be evident that the length of the fronts will change. We can thus conclude that this implies that the refraction coefficient is larger than unity where the length of wave front is decreased and visa versa.

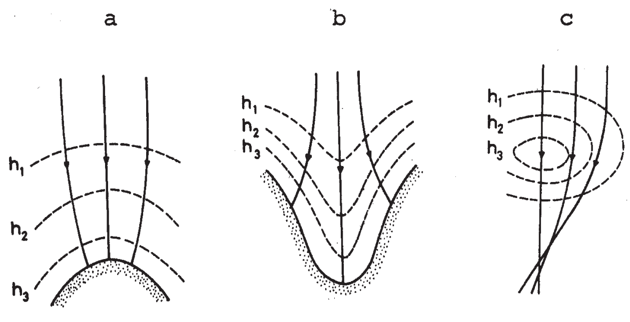

Figure 4.6: Influence of refraction on wave height for three cases. The curves drawn are wave orthogonals and depth contours. a) Increased wave height at a headland due to focusing of energy (converging wave orthogonals). b) Decrease in wave height at bay or fjord (diverging wave orthogaonals). c) Increased wave height behind submerged ridge (converging wave orthogonals).

Figure 4.6 shows that it is a good idea to consider refraction effects when looking for a location for a structure built into the sea. This is the case both if you want small waves (small forces on a structure) or large waves (wave power plant). In fact you will find that many harbours are positioned where you have small waves due to refraction and/or sheltering.

Practically the refraction/shoaling problem is always solved by a large numerical wave propagation model. Examples of such models are D.H.I.'s System21, AaU's MildSim and Delfts freely available SWAN model, just to mention a few of the many models available.

If there is a strong current in an area with waves it can be observed that the current will change the waves as illustrated in Fig. 4.7. The interaction affects both the direction of wave propagation and characteristics of the waves such as height and length. Swell in the open ocean can undergo significant refraction as it passes through major current systems like the Gulf Stream. If the current is in the same direction as the waves the waves become flatter as the wave length will increase. In opposing current conditions the wave length decreases and the waves become steeper. If the wave and current are not co-directional the waves will turn due to the change in phase velocity. The phase velocity is now both a function of the depth and the current velocity and direction. This phenomena is called current refraction. It should be noted that the energy conservation is not valid when the wave propagate through a current field.

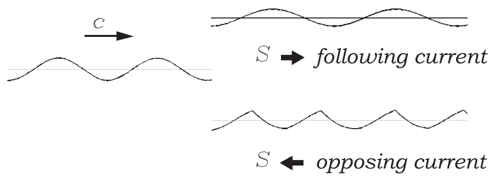

Figure 4.7: Change of wave form due to current.

4.3 Diffraction

If you observe the wave disturbance in a harbour, you will observe wave disturbance also in areas that actually are in shelter of the breakwaters. This wave disturbance is due to the waves will travel also into the shadow of the breakwater in an almost circular pattern of crests with the breakwater head being the center point. The amplitude of the waves will rapidly decrease behind the breakwater. Thus the waves will turn around the head of the breakwater even when we neglect refraction effects. We say the wave diffracts around the breakwater.

If diffraction effects were ignored the wave would propagate along straight orthogonals with no energy crossing the shadow line and no waves would enter into the shadow area behind the breakwater. This is of cause physical impossible as it would lead to a jump in the energy level. Therefore, the energy will spread and the waves diffract.

Figure 4.8: Diffraction around breakwater head.

The wave disturbance in a harbour is determining the motions of moored ships and thus related to both the down-time and the forces in the mooring systems (hawsers and fenders). Also navigation of ships and sediment transport is affected by the diffracted waves. Moreover, diffraction plays a role for forces on offshore large structures and wind mill foundations. It is therefore important to be able to estimate wave diffraction and diffracted wave heights.

From the theory of light we know the diffraction phenomena. As the governing equation for most wave phenomena formally are identical, we can profit from the analytical solution developed for diffraction of electromagnetic waves around a half-infinite screen (Sommerfeld 1896).

Fig. 4.9 shows the change in wave height behind a fully absorbing breakwater. The shown numbers are the so-called diffraction coefficient K_d, which is defined as the diffracted wave height divided by the incident wave height. In reallity a breakwater is not fully absorbing as the energy can either be absorped, transmitted or reflected. For a rubble mound breakwater the main part of the energy is absorbed and most often only a small part of the energy is reflected and transmitted. In case of a vertical breakwater the main part of the energy is reflected. Therefore, these cases are not generally covered by the Sommerfeld

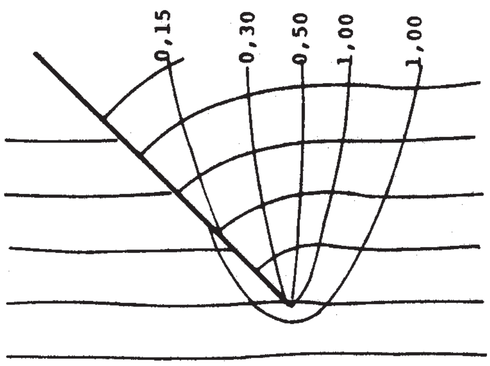

Figure 4.9: Diffraction around absorping breakwater.

solution, but anyway the solution gives an idea of the diffracted wave height.

The preceding description (the Sommerfeld solution) is based on the assumption of constant phase velocity of the wave. As previously derived the phase velocity depends not only on the wave period but also on the water depth. Therefore, we have implicit assumed constant water depth when we apply the Sommerfeld solution.

In the conceptual design of a harbour or another structure is the diffraction diagram is an essential tool. However, a detailed design should be based on either physical model tests or advanced numerical modelling.

A larger mathematical derivation leads to the so-called Mild-Slope equations and Boussinesq equations. It is outside the scope of these notes to present this derivation, but it should just be mentioned that commercial wave disturbance models are based on these equations.

Generally all the shallow water phenomena (i.e. shoaling, refraction and diffraction) are included in such a numerical model. Examples of such models are as previously mentioned D.H.I.'s Mike21, AaU's MildSim and Delfts SWAN model.

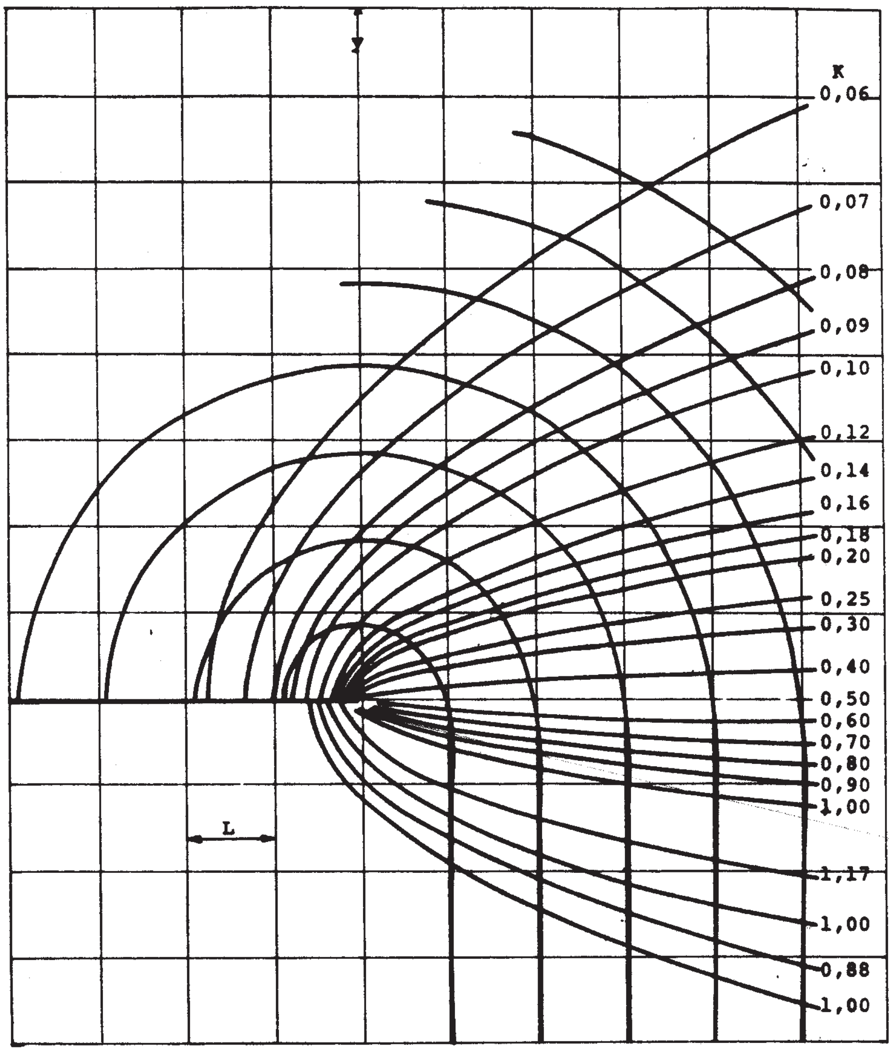

Figure 4.10: Diffraction diagram for fully absorbing breakwater.

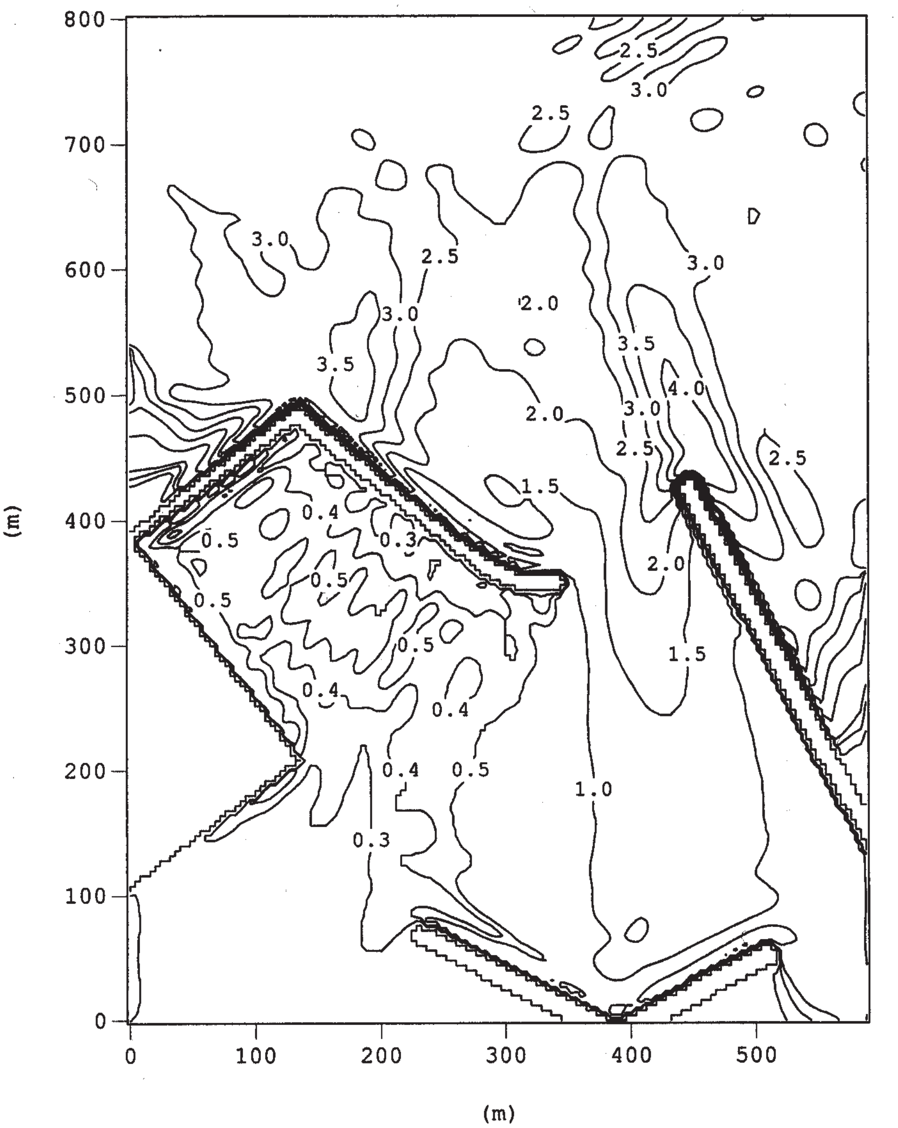

Figure 4.11: Example of wave heights in the outer part of Grenaa harbour calculated by the MildSim model.

4.4 Wave Breaking

Wave measurements during storm periods shows that the wave heights almost never gets higher than approximately 1/10 of the wave length. If we in the laboratory try to generate steep waves we will observe that it is only possible to generate waves with a wave steepness up to between 1/10 and 1/8. If we try to go steeper we will observe that the wave breaks.

Miche (1944) has shown theoretically that the maximum wave is limited by the fact that the particle velocity u cannot be larger then the phase velocity c.

$$u_{max} = c \tag{4.10}$$

The wave steepness is high when the wave breaks and thus the assumptions in the linear theory are violated too strong to give usable results. Miche (1944) found the maximum steepness from Eq. 4.10 to:

$$\frac{H}{L} = 0.142 \cdot tanh(kh) \tag{4.11}$$

If we instead apply the linear theory we get when using the velocity at $z = 0$ a coefficient $1/\pi$ instead of 0.142, which shows that the linear theory is pushed way out of its range of validity.

Eq. 4.11 gives for deep water waves ($\frac{h}{L} \geq \frac{1}{2}$) that the maximum steepness is 0.14. In shallow water ($\frac{h}{L} \leq \frac{1}{20}$) Eq. 4.11 is reduced to:

$$H \leq 0.88 \cdot h \tag{4.12}$$

However, observation shows that this formula is the upper limit and typically the wave breaks around $H/h = 0.6$ to 0.8. In case of irregular waves observations shows that the maximum significant wave height as defined in chapter 5 is around $H_s/h \approx 0.5$.

In reality the breaking wave height depends in shallow water not only on the depth as suggested by Eq. 4.12 but also on the bottom slope. We can observe at least three different wave breaking forms. Waves on deep water breaks by spilling, when the wind has produced relative steep waves.

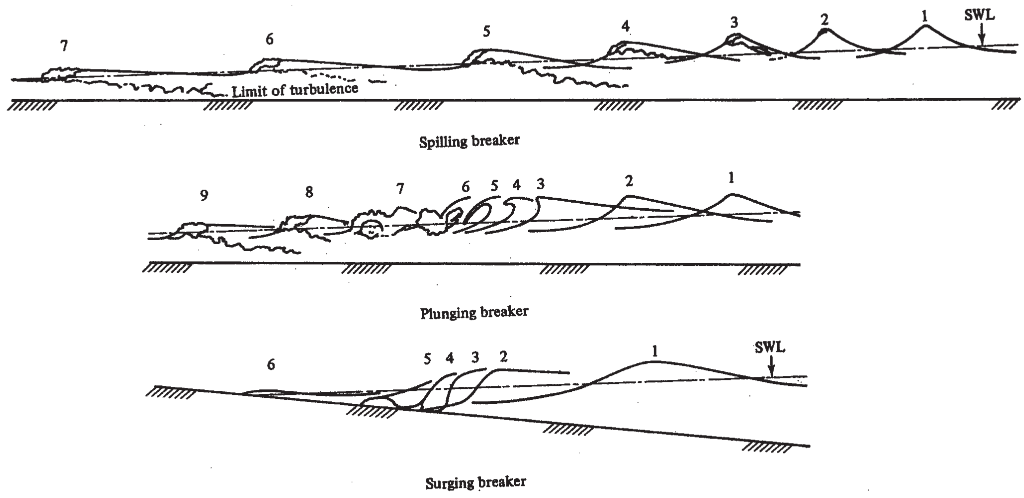

Figure 4.12: Different breaker types.

The type of wave breaking depends on shallow water on both the wave steepness and the bottom slope typically combined in the Iribarren number defined as:

$$\xi = \frac{tan(\alpha)}{\sqrt{H_b/L_0}} = \frac{tan(\alpha)}{\sqrt{s_0}} \tag{4.13}$$

where s_0 is the wave steepness at the breaker point but using the deep water wave length. The Iribarren number is also known as the surf similarity parameter and the breaker parameter. Typical values used for the different breaker types are:

$$\begin{aligned} spilling: &\quad \xi < 0.4 \\ plunging: &\quad 0.4 < \xi < 2.0 \\ surging: &\quad \xi > 2.0 \end{aligned}$$

Fig. 4.13 indicate the breaker type as function of the bottom slope and the wave steepness ($s_0 = H/L_0$) using the above given limits for the breaker parameter. In many cases the reflection from a sloping structure is calculated using the Iribarren number as this determines the breaker process and thus the energy dissipation. Also stability of rubble mound structures depends on the Iribarren number.

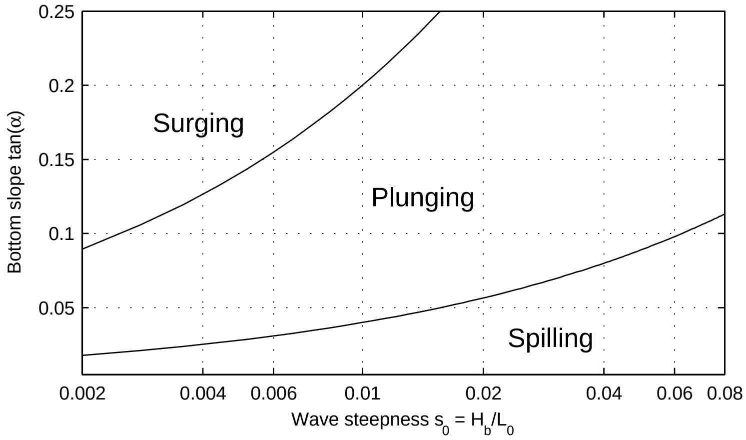

Figure 4.13: Type of wave breaking as function of wave steepness and bottom slope.

Towards the surf zone there are changes in the mean water level. Before the wave breaking point there is a small set-down of the mean water level. From the breaker line and towards the coast line there is a set-up of the water level. These changes in the water level is due to variations in the wave height (wave radiation stress), i.e. before the breaker zone the wave height is increased due to shoaling and causes the set-down. In the breaker zone the wave height is reduced very significantly and leads to set-up, which can be as much as 20% of the water depth at the breaker point.

These water level variation gives also rise to a return flow from the coast towards the breaker zone (cross-shore current). In case of oblique incident waves a long-shore current is also generated. These currents can if they are strong enough be extremely dangerous for swimmers as they occasional can outbreak to the sea and generate what is often refered to as rip currents. Moreover, the wave generated currents are important for the sediment transport at the coast.

Chapter 5

Irregular Waves

5.1 Wind Generated Waves

If you have been at the coast and observed the waves, then it will be obvious that the waves are not regular. The wave field will consist of a mix of different wave heights and lengths. Therefore, it is often necessary to describe a sea state more detailed than possible by the regular waves (H, T).

In the following two sections are described how the water surface can be analyzed by time series analysis in respectively the time domain and frequency domain.

5.2 Time-Domain Analysis of Waves

Definition of the individual wave : Zero-down crossing
The individual wave is defined by two successive zero-down crossings, cf. 5.1. For many years it was common to use zero-up crossings to define a wave, but due to the asymmetry of natural waves, the greatest wave forces are often experienced when the wave front hits a structure. That's one of the main reasons why IAHR (1986) recommended that the height of a wave is defined as the height from a trough to the following crest in a time series. Fig. 5.2

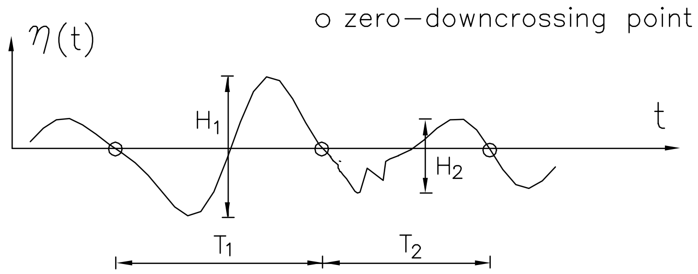

Figure 5.1: Individual waves defined by zero-down crossing.

is an example of surface elevation recordings. The application of zero-down-crossing gives 15 individual waves (N=15). In Table 4.1 the data are arranged according to the descending order of wave height.

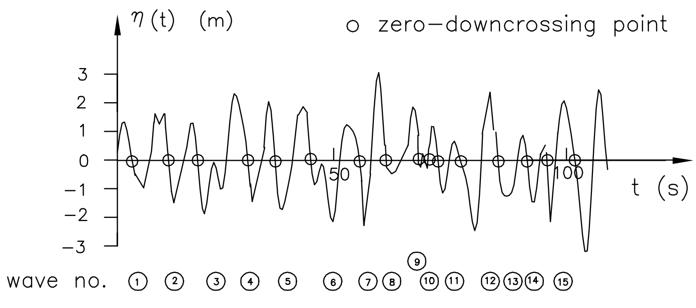

Figure 5.2: Application of zero-down crossing.

Table 4.1. Ranked individual wave heights and corresponding periods in Fig. 5.2.

rank i	1	2	3	4	5	6	7	8	9	10	11	12	13	14	15
H (m)	5.5	4.8	4.2	3.9	3.8	3.4	2.9	2.8	2.7	2.3	2.2	1.9	1.8	1.1	0.23
T (s)	12.5	13.0	12.0	11.2	15.2	8.5	11.9	11.0	9.3	10.1	7.2	5.6	6.3	4.0	0.9
wave no. in 5.2	7	12	15	3	5	4	2	11	6	1	10	8	13	14	9

Characteristic wave heights and periods

Usually a surface elevation recording, exemplified in Fig. 5.2, contains more than several hundred individual waves.

Both wave height and wave period can be considered as random variables, which have certain probability distributions.

Before these distributions are discussed, some definitions of characteristic waves will be given.

Mean wave: $\overline{H}$, $\overline{T}$

$\overline{H}$ and $\overline{T}$ are the mean values of the heights and periods , respectively, of all individual waves. Table 4.1 yields

$$\overline{H} = \frac{1}{15} \sum_{i=1}^{15} H_i = 2.9 \text{ m} \qquad \overline{T} = \frac{1}{15} \sum_{i=1}^{15} T_i = 9.25 \text{ s}$$

Root-mean-square wave: H_{rms}

This wave has a height defined as

$$H_{rms} = \sqrt{\frac{1}{N} \sum_{i=1}^{N} H_i^2}$$

From Table 4.1 is found

$$H_{rms} = \sqrt{\frac{1}{15} \sum_{i=1}^{15} H_i^2} = 3.20 \text{ m}$$

Significant wave: H_s, T_s or $H_{1/3}$, $T_{H_{1/3}}$

The significant wave height is the average of the wave heights of the one-third highest waves. The significant wave period is the average of the wave periods of the one-third highest waves. From Table 4.1 one finds

$$H_s = \frac{1}{5} \sum_{i=1}^{5} H_i = 4.44 \text{ m} \qquad T_s = \frac{1}{5} \sum_{j=1}^{5} T_j = 12.9 \text{ s} \qquad i, j \text{ are the rank no.}$$

The significant wave is very often used as the design wave. The reason might be that in old days structures were designed an a basis of visually observed waves. Experiences show that often the wave height and period reported by visual observation correspond approximately to the measured significant wave. Therefore the choice of significant wave as design wave can make use of the existing engineering experience.

Maximum wave: H_{max}, $T_{H_{max}}$
This is the wave, which has the maximum wave height. In Table 4.1,

$$H_{max} = 5.5 \text{ m} \qquad\qquad T_{H_{max}} = 12.5 \text{ s}$$

Note, however, that H_{max} is a random variable which depends on the number of individual waves in the time series.
The maximum wave from a long time series corresponding to a storm with a return period of e.g. 100 years is often chosen as the design wave for structures which are very important and very sensitive to wave loads.

Highest one-tenth wave: $H_{1/10}$, $T_{H_{1/10}}$
$H_{1/10}$ is the average of the wave heights of the one-tenth highest waves. $T_{H_{1/10}}$ is the average of the wave periods of the one-tenth highest wave.

Wave height with exceedence probability of $\alpha\%$: $H_{\alpha\%}$
It is often practical to denote a wave height according to the probability of exceedence. Examples are $H_{0.1\%}$, $H_{1\%}$, $H_{2\%}$ etc. In many situations $H_{0.1\%}$ in the 100 year storm is used as the design wave.

Distribution of individual wave heights

Histogram of wave heights

Instead of showing all individual wave heights, it is easier to use the wave height histogram which gives information about the number of waves in various wave height intervals. Fig. 5.3 is the histogram of wave heights corresponding to Table 4.1.

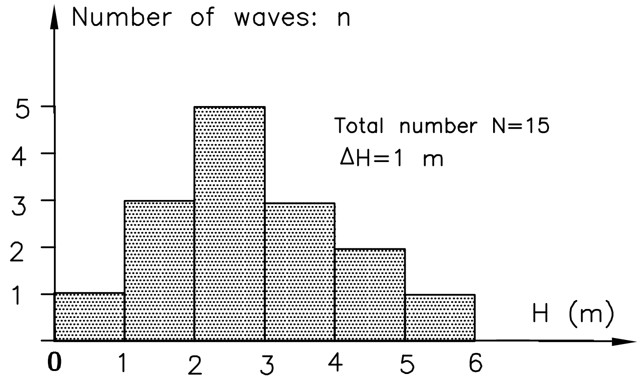

Figure 5.3: Wave height histogram.

Non-dimensionalized histogram

In order to compare the distribution of wave heights at different locations, the histogram of wave heights is non-dimensionalized, cf. Fig. 5.4.

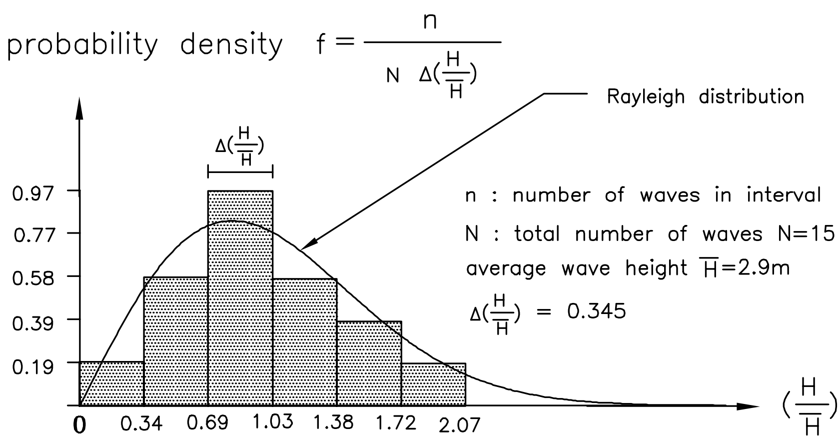

Figure 5.4: Non-dimensionalized wave height histogram.

When $\Delta(H/\overline{H})$ approaches zero, the probability density becomes a smooth curve. Experience and theory have shown that this curve is very close to the Rayleigh distribution in case of deep water waves. In other words, the individual wave heights follow the Rayleigh distribution.

Rayleigh distribution

The Rayleigh probability density function is defined as

$$f(x) \;=\; \frac{\pi}{2}\, x\, \exp\left(-\frac{\pi}{4}x^2\right) \qquad \text{where} \qquad x = \frac{H}{\overline{H}} \tag{5.1}$$

The Rayleigh distribution function is

$$F(x) \;=\; \text{Prob}\{X < x\} \;=\; 1 \;-\; \exp\left(-\frac{\pi}{4}x^2\right) \tag{5.2}$$

Relation between characteristic wave heights

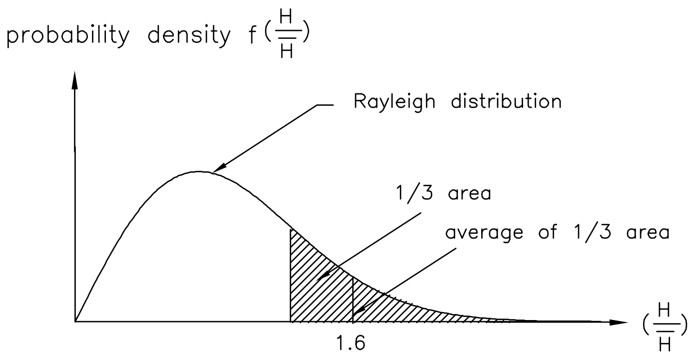

Figure 5.5: Relation between H_s and $\overline{H}$.

If we adopt the Rayleigh distribution as an approximation to the distribution of individual wave heights, then the characteristic wave heights $H_{1/10}$, $H_{1/3}$, H_{rms} and $H_{\alpha\%}$ can be expressed by $\overline{H}$ through the manipulation of the Rayleigh probability density function.

$$\begin{aligned} H_{1/10} &= 2.03\,\overline{H} \\ H_{1/3} &= 1.60\,\overline{H} \\ H_{rms} &= 1.13\,\overline{H} \\ H_{2\%} &= 2.23\,\overline{H} \\ H_{0.1\%} &= 2.97\,\overline{H} \end{aligned} \tag{5.3}$$

Fig. 5.5 illustrates how to obtain the relation between H_s and $\overline{H}$.

The Rayleigh distribution function given by H_s instead of $\overline{H}$ reads

$$F(H) \;=\; 1 \;-\; \exp\left(-2\left(\frac{H}{H_s}\right)^2\right) \tag{5.4}$$

Individual wave height distribution in shallow water

Only in relatively deep water, the Rayleigh distribution is a good approximation to the distribution of individual wave heights. When wave breaking takes place due to limited water depth, the individual wave height distribution will differ from the Rayleigh distribution.

Stive (1986), proposed the following empirical correction to the Rayleigh distribution based on model tests and also roughly checked against some prototype data.

$$H_{1\%} \;=\; H_{m0}\left(\frac{ln100}{2}\right)^{\frac{1}{2}}\left(1+\frac{H_{m0}}{h}\right)^{-\frac{1}{3}} \tag{5.5}$$

$$H_{0.1\%} \;=\; H_{m0}\left(\frac{ln1000}{2}\right)^{\frac{1}{2}}\left(1+\frac{H_{m0}}{h}\right)^{-\frac{1}{2}} \tag{5.6}$$

where h is the water depth, $H_{1\%}$ means the 1% exceedence value of the wave height determined by zero-down-crossing analysis, whereas the significant wave height H_{m0} is determined from the surface elevataion spectrum, cf. section 5.3. The correction formulae are very useful for checking the wave height distribution in small scale physical model tests, cf. Fig. 5.6.

Klopmann et al. (1989) proposed also a semi-empirical expression for the individual wave height distribution. Worth mentioning is also the very much used method of Battjes and Groenendijk (2000) which was calibrated against a lot of physical model test data, but the numerical procedure is somewhat more complicated.

Section 5.3 gives a more detailed discussion on the validity of the Rayleigh distribution, based on energy spectrum width parameter.

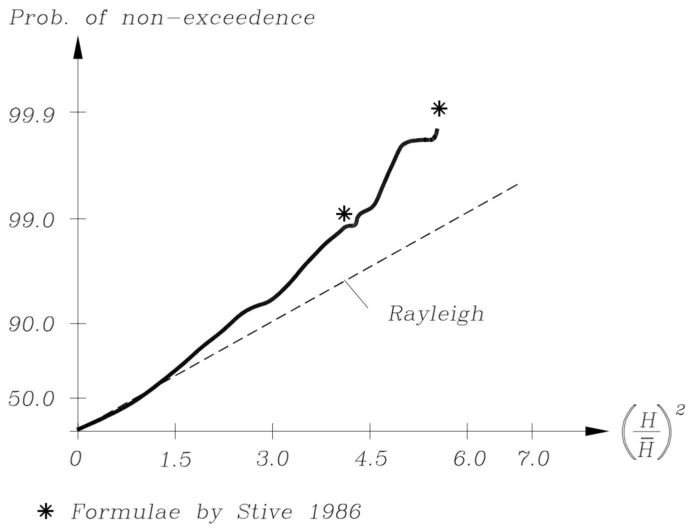

Figure 5.6: Comparison of the expression by Stive, 1986, for shallow water wave height distribution with model test results. Aalborg University Hydraulics Laboratory 1990.

Maximum wave height H_{max}

As mentioned above H_{max} is a random variable that depends on the number of waves in the timeseries. Below some facts about the distribution of H_{max} are given.

<u>Distribution of H_{max}</u>

The distribution function of $X = H/\overline{H}$ is the Rayleigh distribution

$$F_X(x) \;=\; \text{Prob}\{X < x\} \;=\; 1 \;-\; \exp\left(-\frac{\pi}{4}x^2\right) \tag{5.7}$$

If there are N individual waves in a storm[1], the distribution function of $X_{max} = H_{max}/\overline{H}$ is

$$\begin{aligned} F_{X_{max}}(x) \;&=\; \text{Prob}\{X_{max} < x\} \;=\; (\; F_X(x)\;)^N \\ &=\; \left(\; 1 \;-\; \exp\left(-\frac{\pi}{4}x^2\right)\;\right)^N \end{aligned} \tag{5.8}$$

Note that $F_{X_{max}}(x)$ can be interpreted as the probability of the non-occurrence of the event ($X > x$) in any of N independent trials. The probability density

[1] A storm usually lasts some days. The significant wave height is varying during a storm. However we are more interested in the maximum significant wave height in a short period of time. In practice, N is often assumed to be 1000.

function of X_{max} is

$$f_{X_{max}}(x) = \frac{\mathrm{d}F_{X_{max}}}{\mathrm{d}x} = \frac{\pi}{2}\; N\; x\; \exp\left(-\frac{\pi}{4}x^2\right) \left(1 \;-\; \exp\left(-\frac{\pi}{4}x^2\right)\right)^{N-1} \tag{5.9}$$

The density function of X and the density function of X_{max} are sketched in Fig. 5.7.

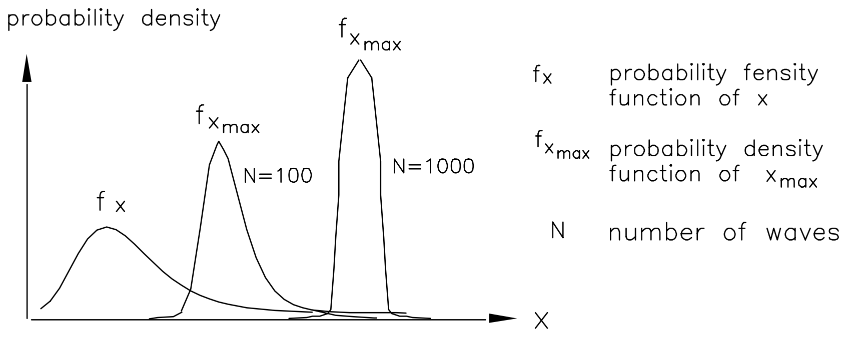

Figure 5.7: Probability density function of X and X_{max}.

Mean, median and mode of H_{max}

Mean, median and mode are often used as the characteristic values of a random variable. Their definitions are given in Fig. 5.8.

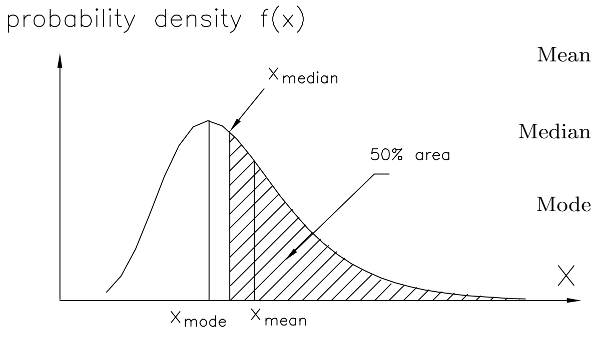

Mean $\quad x_{mean} = E[X] = \int_{-\infty}^{+\infty} x f_X(x)\mathrm{dx}$

Median $\quad x_{median} = x\Big|_{F_X(x)=0.5}$

Mode $\quad x_{mode} = x\Big|_{f_X(x)=max}$

Figure 5.8: Probability density function of X and X_{max}.

By putting eqs (5.8) and (5.9) into the definitions, we obtain

$$(H_{max})_{mean} \approx \left(\sqrt{\frac{\ln N}{2}} + \frac{0.577}{\sqrt{8\;\ln N}}\right) H_s \tag{5.10}$$

$$(H_{max})_{mode} \approx \sqrt{\frac{\ln N}{2}}\, H_s \tag{5.11}$$

Furthermore, $(H_{max})_\mu$, defined as the maximum wave height with exceedence probability of μ (cf. Fig. 5.9), is

$$(H_{max})_\mu \approx \sqrt{\frac{1}{2}\, \ln\left(\frac{N}{\ln\left(\frac{1}{1-\mu}\right)}\right)}\, H_s \tag{5.12}$$

Obviously $(H_{max})_{median} = (H_{max})_{0.5}$.
We get for the commonly used $N = 1000$ the following maximum wave heights:

$$(H_{max})_{mode} \approx 1.86 H_s = 2.97\overline{H} \tag{5.13}$$

$$(H_{max})_{mean} \approx 1.94 H_s = 3.10\overline{H} \tag{5.14}$$

$$(H_{max})_{10\%} \approx 2.14 H_s = 3.42\overline{H} \tag{5.15}$$

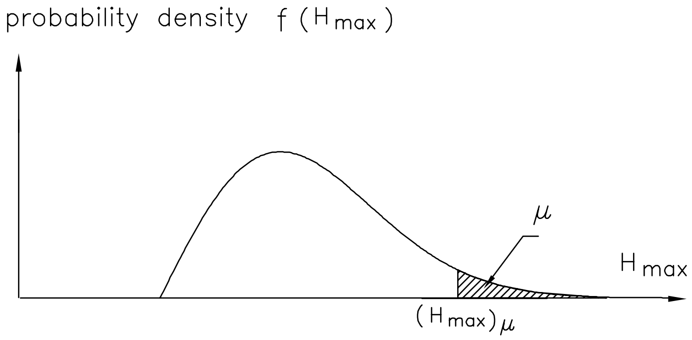

Figure 5.9: Definition of $(H_{max})_\mu$.

Monte-Carlo simulation of H_{max} distribution

The distribution of H_{max} can also be studied by the Monte-Carlo simulation. Individual wave heights follow the Rayleigh distribution

$$F(H) = 1 - exp\left(-2 \left(\frac{H}{H_s}\right)^2 \right) \tag{5.16}$$

The storm duration corresponds to N individual waves.

1) Generate randomly a data between 0 and 1. Let the non-exceedence probability $F(H)$ equal to that data. One individual wave height H is obtained by (cf. Fig. 5.10)

$$H = F^{-1}(F(H)) = H_s \sqrt{\frac{-\ln(1 - F(H))}{2}} \tag{5.17}$$

2) Repeat step 1) N times. Thus we obtain a sample belonging to the distribution of eq (5.16) and the sample size is N.

3) Pick up H_{max} from the sample.

4) Repeat steps 2) and 3), say, 10,000 times. Thus we get 10,000 values of H_{max}.

5) Draw the probability density of H_{max}.

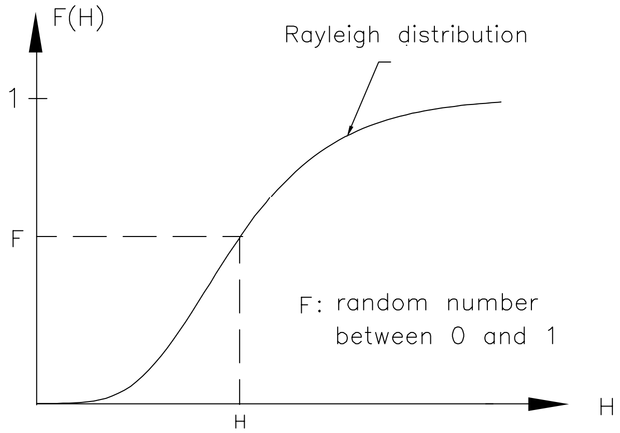

Figure 5.10: Simulated wave height from the Rayleigh distribution.

Distribution of wave periods
It is summarized as

- When we talk about the distribution of wave periods, we often mean the joint distribution of significant wave height and significant wave period. Until now there is no general theoretical expression for the joint distribution, even though there are some so-called *scatter diagrams* based on wave recording. Such a diagram is valid only for the measurement location. The relation between H_s and T_s is often simplified as $T_s = \alpha H_s^\beta$, e.g. in Canadian Atlantic waters $\alpha = 4.43$ and $\beta = 0.5$ (Neu 1982).
- The distribution of wave periods is narrower than that of wave height.
- The empirical relation $T_{max} \approx T_{1/10} \approx T_{1/3} \approx 1.2\ \overline{T}$ (Goda 1985).

5.3 Frequency-Domain Analysis

The concept of a spectrum can be attributed to Newton, who discovered that sunlight can be decomposed into a spectrum of colors from red to violet, based on the principle that white light consists of numerous components of light of various colors (wave length or wave frequency).

Energy spectrum means the energy distribution over frequency. Spectral analysis is a technique of decomposing a complex physical phenomenon into individual components with respect to frequency.

Spectral analysis of irregular waves is very important for the design of structures. For example, in the oil-drilling platform design where wave forces plays an important role, it is of importance to design the structure in such a way that the natural frequency of the structure is rather far away from the frequency band where the main part of wave energy concentrates. In this way resonance phenomenon and the corresponding dynamic amplification of force and deformation can be avoided.

Some basic concepts of linear wave theory

Surface elevation

The surface elevation of a linear wave is:

$$\eta(x,t) = \frac{H}{2}\cos(\omega t - kx + \delta) = a\ \cos(\omega t - kx + \delta) \tag{5.18}$$

where	H	wave height
	a	amplitude, $a = H/2$
	ω	angular frequency, $\omega = 2\pi/T$
	T	wave period.
	k	wave number, $k = 2\pi/L$
	L	wave length
	δ	initial phase

We can also define the observation location to $x = 0$ and obtain

$$\eta(t) = a\ \cos(\omega t + \delta) \tag{5.19}$$

The relation between wave period and wave length (dispersion relationship) is

$$L = \frac{g\,T^2}{2\pi}\ \tanh\left(\frac{2\pi h}{L}\right) \tag{5.20}$$

where h is water depth.

Wave energy

The average wave energy per unit area is:

$$E = \frac{1}{8}\rho\ g\ H^2 = \frac{1}{2}\rho\ g\ a^2 \quad (\text{Joule/m}^2 \text{ in SI unit}) \tag{5.21}$$

Variance of surface elevation of a linear wave

The variance of the surface elevation of a sinus wave is:

$$\begin{aligned}
\mathrm{Var}[\eta(t)] &= E\left[\left(\eta(t) - \overline{\eta(t)}\right)^2\right] && \text{(E: Expectation)}\\
&= E\left[\left(\eta(t)\right)^2\right]\\
&= \tfrac{1}{T}\int_0^T \eta^2(t)\ \mathrm{dt} && \text{(T: wave period)}\\
&= \tfrac{1}{2}\ a^2
\end{aligned}$$

Superposition of linear waves

Since the governing equation (Laplace equation) and boundary conditions are linear in small amplitude wave theory, it is known from mathematics that small amplitude waves are superposable. This means that the superposition of a number of linear waves with different wave height and wave period will be:

	superposition		wave 1		wave 2		$\cdots$		wave N
velocity potential	φ	=	φ_1	+	φ_2	+	$\cdots$	+	φ_N
surface elevation	η	=	η_1	+	η_2	+	$\cdots$	+	η_N
particle velocity	u	=	u_1	+	u_2	+	$\cdots$	+	u_N
dynamic pressure	p	=	p_1	+	p_2	+	$\cdots$	+	p_N

Example of variance spectrum

First we will make use of an example to demonstrate what a variance spectrum is.

Surface elevation of irregular wave

Fig. 5.11 gives an example of an irregular wave surface elevation which is constructed by adding 4 linear waves (component waves) of different wave height and wave period. The superposed wave surface elevation is

$$\eta(t) \;=\; \sum_{i=1}^{4} \eta_i(t) \;=\; \sum_{i=1}^{4} a_i \;\cos(\omega_i t + \delta_i) \tag{5.22}$$

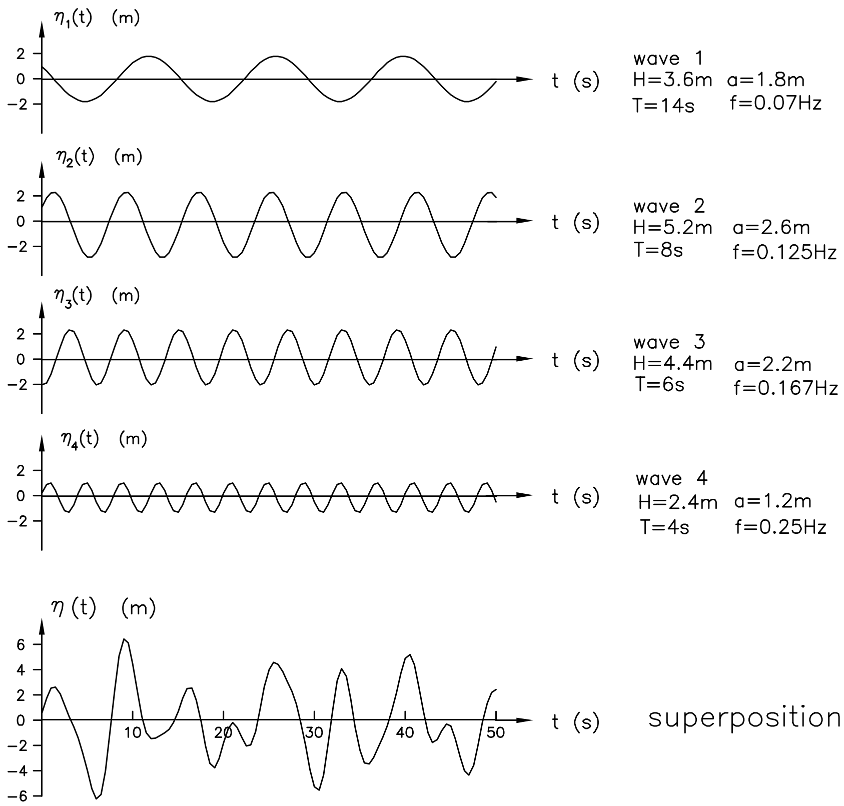

Figure 5.11: Simulation of irregular waves by superposition of linear waves.

Variance diagram

Instead of Fig. 5.11,we can use a variance diagram, shown in Fig. 5.12, to describe the irregular wave.

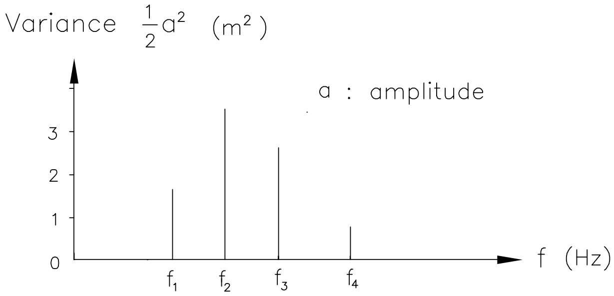

Figure 5.12: Variance diagram.

In comparison with Fig. 5.11, the variance diagram keeps the information on amplitude (a_i) and frequency (f_i, hence T_i and L_i) of each component, while the information on initial phase (δ_i) is lost. This information loss does not matter because the surface elevation of irregular wave is a random process. We can simply assign a random initial phase to each component.

Variance spectral density $S_\eta(f)$

The variance diagram can be converted to variance spectrum, The spectral density is defined as

$$S_\eta(f) = \frac{\frac{1}{2}a^2}{\Delta f} \qquad (\mathrm{m}^2\ \mathrm{s}) \tag{5.23}$$

where Δf is the frequency band width[2], cf. Fig. 5.13.

[2]we will see later that Δf depends on signal recording duration. In the figure it is assumed that $\Delta f = 0.01Hz$

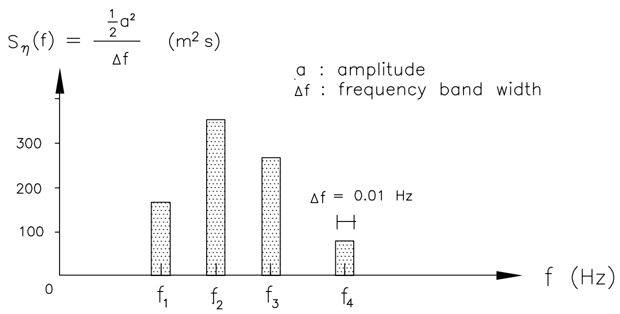

Figure 5.13: Stepped Variance spectrum.

In reality an irregular wave is composed of infinite number of linear waves with different frequency. Fig. 5.14 gives an example of stepped variance spectrum. When Δf approaches zero, the variance spectrum becomes a continuous curve.

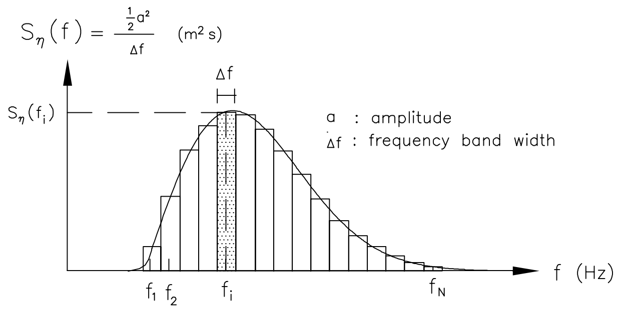

Figure 5.14: Continuous variance spectrum (wave energy spectrum).

A variance spectrum is also called energy spectrum. But strictly speaking, the energy spectral density should be defined as

$$S(f) \;=\; \frac{\frac{1}{2}\rho\ g\ a^2}{\Delta f} \qquad (\tfrac{J\ s}{m^2}) \tag{5.24}$$

Construction of time series from variance spectrum

We can also construct time series of surface elevation from variance spectrum. In Fig. 5.14 the known variance spectral density $S_\eta(f)$ is divided into N parts by the frequency band width Δf. This means that the irregular wave is composed of N linear waves

$$\eta(t) \;=\; \sum_{i=1}^{N} \eta_i(t) \;=\; \sum_{i=1}^{N}\ a_i\ \cos(\omega_i t + \delta_i) \tag{5.25}$$

The variance of each linear wave is

$$S_\eta(f_i)\ \Delta f \ = \ \frac{1}{2}a_i^2 \qquad i = 1, 2, \cdots, N \tag{5.26}$$

Therefore the amplitude is

$$a_i \ = \ \sqrt{2\ S_\eta(f_i)\ \Delta f} \qquad i = 1, 2, \cdots, N \tag{5.27}$$

The angular frequency is

$$\omega_i \ = \ \frac{2\pi}{T_i} \ = \ 2\pi f_i \qquad i = 1, 2, \cdots, N \tag{5.28}$$

The initial phase δ_i is assigned a random number between 0 and 2π. Hence by use of Eq. (5.25) we can draw the time-series of the surface elevation of the irregular wave which has the variance spectrum as shown in Fig. 5.14.

Fourier series

Conversion of irregular surface elevation into variance spectrum is not as simple as the above example, where the linear components of the irregular wave are pre-defined (cf. Fig. 5.11). We need to decompose the irregular wave into its linear components. First let's see how it can be done with a known continuous function $x(t)$.

Fourier series is used to represent any arbitrary function[3].

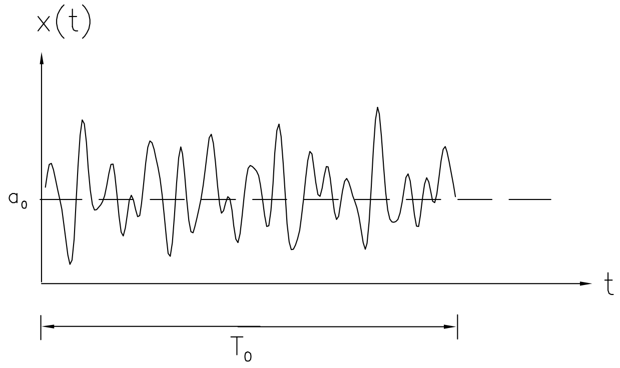

Figure 5.15: Arbitrary periodic function of time.

$$
\begin{aligned}
x(t) &= a_0 + \sum_{i=1}^{\infty}\left(a_i \cos\left(\frac{2\pi i}{T_0}t\right) + b_i \sin\left(\frac{2\pi i}{T_0}t\right)\right) \\
&= \sum_{i=0}^{\infty}\left(a_i \cos\omega_i t + b_i \sin\omega_i t\right)
\end{aligned} \tag{5.29}
$$

where a_i and b_i are Fourier coefficients given by

$$
\begin{aligned}
a_0 &= \tfrac{1}{T_0}\int_0^{T_0} x(t)\ \mathrm{dt} \quad \text{and} \quad b_0 = 0 \\
\left.\begin{aligned}
a_i &= \tfrac{2}{T_0}\int_0^{T_0} x(t)\ \cos\omega_i t\ \mathrm{dt} \\
b_i &= \tfrac{2}{T_0}\int_0^{T_0} x(t)\ \sin\omega_i t\ \mathrm{dt}
\end{aligned}\right\} &\quad i = 1, 2, 3, \cdots, \infty
\end{aligned} \tag{5.30}
$$

[3]Not all mathematicians agree that an arbitrary function can be represented by a Fourier series. However, all agree that if $x(t)$ is a periodic function of time t, with period T_0 then $x(t)$ can be expressed as a Fourier series. In our case $x(t)$ is the surface elevation of irregular wave, which is a random process. if T_0 is large enough, we can assume that $x(t)$ is a periodic function with period T_0.

Physical interpretation

Now we say that the continuous function $x(t)$ is the surface elevation of irregular wave. $\eta(t)$ can be expanded as a Fourier series.

$$\eta(t) \;=\; \sum_{i=0}^{\infty} (a_i \cos\omega_i t \;+\; b_i \sin\omega_i t)$$

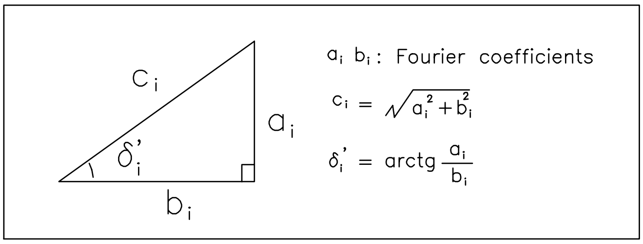

$$\begin{aligned}
&= \sum_{i=0}^{\infty} \Big(c_i \sin\delta_i' \;\cos\omega_i t \;+\; c_i \cos\delta_i' \;\sin\omega_i t \Big) \\
&= \sum_{i=0}^{\infty} c_i (\sin\delta_i' \;\cos\omega_i t \;+\; \cos\delta_i' \;\sin\omega_i t) \\
&= \sum_{i=0}^{\infty} c_i \;\sin(\omega_i t \;+\; \delta_i' \,) \\
&= \sum_{i=0}^{\infty} c_i \;\cos(\omega_i t \;+\; \delta_i \,) \qquad (5.31)
\end{aligned}$$

where $\delta_i = \delta_i' - \frac{\pi}{2}$ and $\sin(x+y) = \sin(x)\cos(y) + \cos(x)\sin(y)$ have been used. That is to say, any irregular wave surface elevation, expressed as a continues function, is composed of infinite number of linear waves with

$$\left.\begin{array}{lll} \text{amplitude} & c_i \;=\; \sqrt{a_i^2 + b_i^2} \\ \text{period} & T_i \;=\; \frac{2\pi}{\omega_i} \;=\; \frac{T_0}{i} \end{array}\right\} \quad i = 0, 1, \cdots, \infty \qquad (5.32)$$

$\{a_i,\ b_i\},\ i = 0, 1, 2, \cdots, \infty$, are given in Eq. (5.30).

Discrete signal analysis

The measurement of surface elevation is carried out digitally. We do not have, neither necessary, a continuous function of the surface elevation. Instead we have a series of surface elevation measurement equally spaced in time, cf. Fig. 5.16.

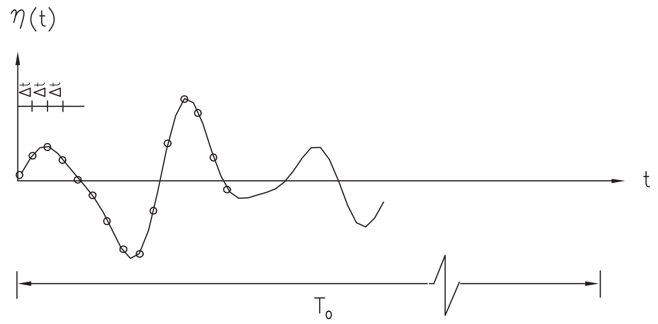

Figure 5.16: Sampling of surface elevation at regular intervals.

If the sampling frequency is f_s, then the time interval between two succeeding points is $\Delta t = 1/f_s$. Corresponding to the sample duration T_0 the total number of sample is $N = T_0/\Delta t$. Thus we obtain a discrete time series of surface elevation

$$\eta_0, \quad \eta_1, \quad \cdots, \quad \eta_{N-1}$$

The Fourier coefficients

$$(a_0,\ b_0), \quad (a_1,\ b_1), \quad \cdots, \quad (a_{N-1},\ b_{N-1})$$

can be obtained by Fast Fourier Transforms (FFT)[4]. That is to say, the irregular wave surface elevation, expressed by digital time series, is composed of N linear waves

$$\eta(t) \;=\; \sum_{i=0}^{N-1} \eta_i(t) \;=\; \sum_{i=0}^{N-1} \sqrt{a_i^2 + b_i^2}\ \cos(\omega_i t + \delta_i) \tag{5.33}$$

$$\left.\begin{array}{ll} \text{amplitude} & \sqrt{a_i^2 + b_i^2} \\ \text{angular frequency} & \omega_i \;=\; \frac{2\pi i}{T_0} \\ \text{period} & T_i \;=\; \frac{2\pi}{\omega_i} \;=\; \frac{T_0}{i} \\ \text{frequency} & f_i \;=\; \frac{1}{T_i} \;=\; \frac{i}{T_0} \end{array}\right\} \quad i = 0, 1, \cdots, N-1 \tag{5.34}$$

[4]FFT is a computer algorithm for calculating DFT. It offers an enormous reduction in computer processing time. For details of DFT and FFT, refer to Newland (1975)

Therefore we obtain the variance spectrum

$$\begin{aligned} \text{frequency width} \qquad \Delta f &= f_{i+1} - f_i = \frac{1}{T_0} \\ \text{spectral density} \qquad S_\eta(f_i) &= \frac{\frac{1}{2}(amplitude)^2}{\Delta f} = \frac{\frac{1}{2}(a_i^2 + b_i^2)}{\Delta f} \end{aligned} \tag{5.35}$$

An example of variance spectrum is shown in Fig. 5.17.

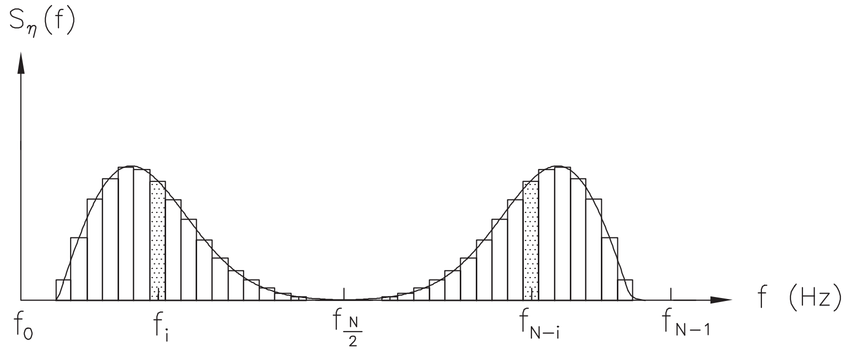

Figure 5.17: Variance spectrum.

Nyquist frequency $f_{nyquist}$

Nyquist frequency $f_{nyquist}$ is the maximum frequency which can be detected by the Fourier analysis.

Fourier analysis decomposes N digital data into N linear components. The frequency of each component is

$$f_i = \frac{i}{T_0} \qquad i = 0, 1, \cdots, N-1 \tag{5.36}$$

The Nyquist frequency is

$$f_{nyquist} = f_{\frac{N}{2}} = \frac{\frac{N}{2}}{T_0} = \frac{\frac{1}{2}\frac{T_0}{\Delta}}{T_0} = \frac{f_s}{2} \tag{5.37}$$

where f_s sample frequency

Δ time interval between two succeeding sample points, $\Delta = 1/f_s$

T_0 sample duration

N total number of sample, $N = T_0/\Delta$

The concept of Nyquist frequency means that the Fourier coefficients $\{ a_i, \ b_i \}$, $i = 0, 1, \cdots, N-1$, contains two parts, the first half part below the Nyquist frequency ($i = 0, 1, \cdots, N/2-1$) represents true components while the second half part ($i = N/2, N/2+1, \cdots, N-1$) is the folding components (aliasing).

Fig. 5.18 gives an example on aliasing after the Fourier analysis of discrete time series of a linear wave.

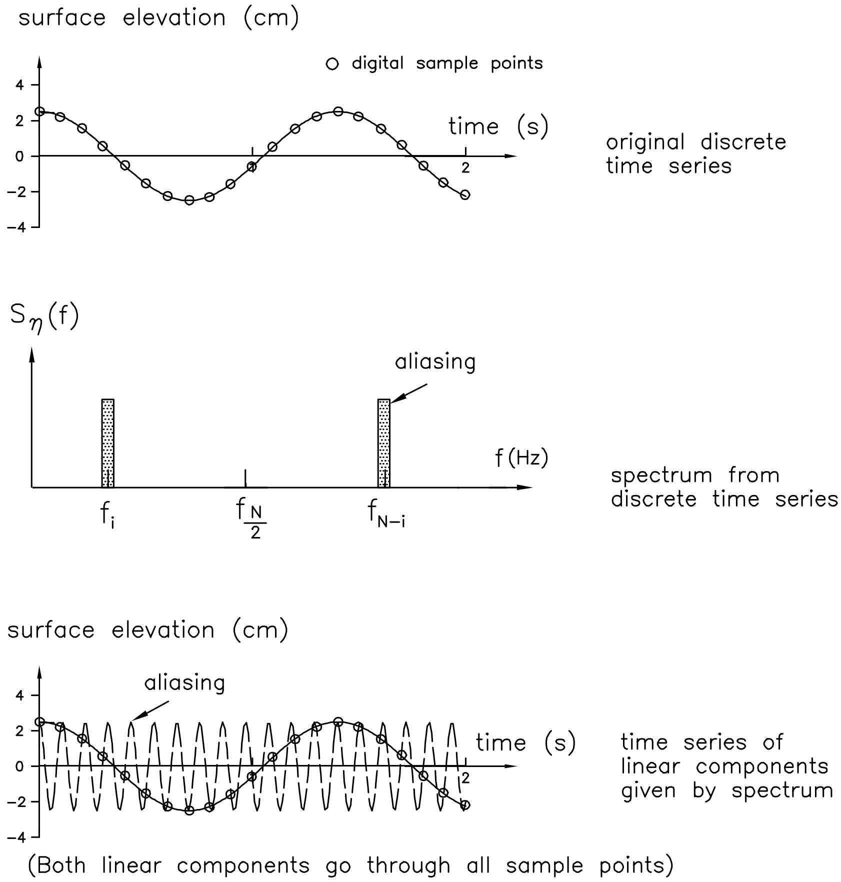

Figure 5.18: Aliasing after Fourier analysis.

The solution to aliasing is simple: let $\{ a_i,\ b_i \}$, $i = N/2, N/2+1, \cdots, N-1$, equal to zero, cf. Fig. 5.19. That is the reason why $f_{nyquist}$ is also called cut-off frequency. In doing so we are actually assuming that irregular wave contains no linear components whose frequency is higher than $f_{nyquist}$. This assumption can be assured by choosing sufficiently high sample frequency f_s in combination with an analog low-pass filter, cf. Eq. 5.37.

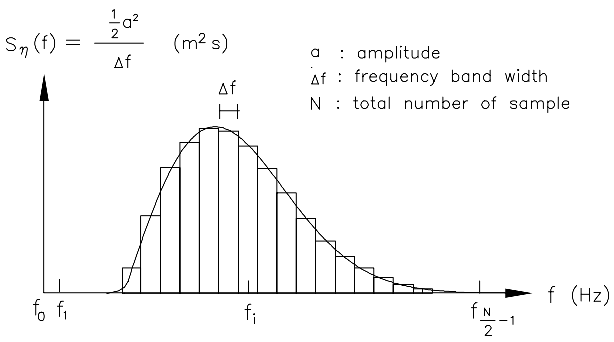

Figure 5.19: Variance spectrum after cut-off (refer to Fig. 5.17).

Taper data window

Fourier analysis requires that $\eta(t)$ is a periodic function with period T_0, it may be desirable to modify the recorded time series before Fourier analysis, so that the signal looks like a periodic function. The modification is carried out with the help of taper data window.

The widely-used cosine taper data window reads

$$d(t) \quad = \quad \begin{cases} \frac{1}{2}\left(1 - \cos\frac{10\pi t}{T_0}\right) & 0 \leq t \leq \frac{T_0}{10} \\ 1 & \frac{T_0}{10} \leq t \leq \frac{9T_0}{10} \\ \frac{1}{2}\left(1 + \cos\frac{10\pi\left(t - \frac{9T_0}{10}\right)}{T_0}\right) & \frac{9T_0}{10} \leq t \leq T_0 \end{cases} \tag{5.38}$$

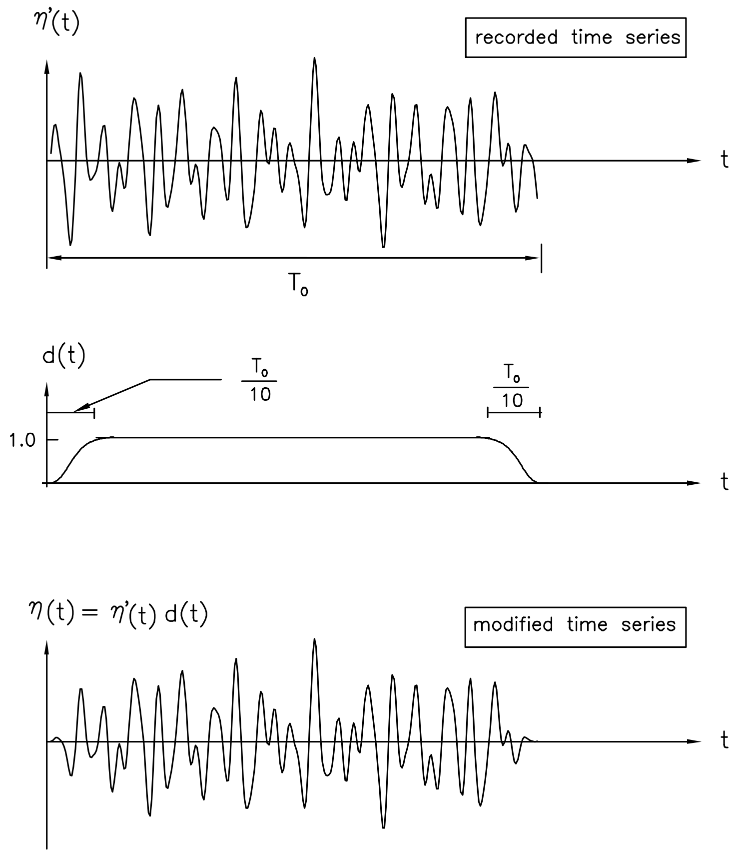

Figure 5.20: Taper data window.

Characteristic wave height and period

The variance spectrum, illustrated in Fig. 5.21, says nothing about how high the individual waves will be. Now we will see how to estimate the characteristic wave height and period based on the variance spectrum.

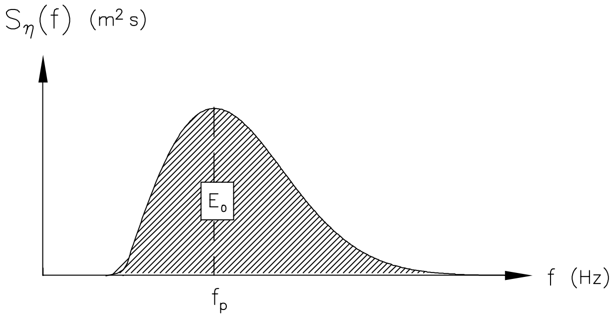

Figure 5.21: Variance spectrum.

n order moment m_n

m_n is defined as

$$m_n \;=\; \int_0^\infty f^n\; S_\eta(f)\; \mathrm{df} \tag{5.39}$$

The zero moment is

$$m_0 \;=\; \int_0^\infty S_\eta(f)\; \mathrm{df} \tag{5.40}$$

which is actually the area under the curve, cf. Fig. 5.21.

Spectrum width parameter and validity of the Rayleigh distribution

From the definition of m_n, it can be seen that the higher the order of moment, the more weight is put on the higher frequency portion of the spectrum. With the same m_0, a wider spectrum gives larger values of the higher order moment ($n \geq 2$). Longuet-Higgins has defined a spectrum width parameter

$$\varepsilon \;=\; \sqrt{1 \;-\; \frac{m_2^2}{m_0 m_4}} \tag{5.41}$$

It has been proven theoretically that

spectrum width parameter		wave height distribution
$\varepsilon = 0$	narrow spectrum	Rayleigh distribution
$\varepsilon = 1$	wide spectrum	Normal distribution

In reality ε lies in the range of 0.4-0.5. It has been found that Rayleigh distribution is a very good approximation and furthermore conservative, as the Rayleigh distribution gives slightly larger wave height for any given probability level.

Significant wave height H_{m_0} and peak wave period T_p

When wave height follows the Rayleigh distribution, i.e. $\varepsilon = 0$, the significant wave height H_s[5] can theoretically be expressed as

$$H_s \approx H_{m_0} \ \equiv \ 4 \ \sqrt{m_0} \tag{5.42}$$

In reality where $\varepsilon = 0.4 - 0.5$, a good estimate of significant wave height from energy spectrum is

$$H_s \ = \ 3.7 \ \sqrt{m_0} \tag{5.43}$$

Peak frequency is defined as (cf. Fig. 5.21)

$$f_p \ = \ f\Big|_{S_\eta(f)=max} \tag{5.44}$$

Wave peak period ($T_p = 1/f_p$) is approximately equal to significant wave period defined in time-domain analysis.

[5] H_{m_0} denotes a wave height determined from spectrum while H_s or $H_{1/3}$ is significant wave height determined from time-domain analysis. They are equal to each other when wave height follows the Rayleigh distribution.

Chapter 6

References

Battjes, J. A. and Groenendijk, H. W.
Wave height distributions on shallow foreshores.
Coastal Engineering, Vol. 40, 2000, pp. 161-182.

Brorsen, Michael, 2007.
Lecture Notes on Fluid Mechanics.
Department of Civil Engineering, Aalborg University.

Burcharth, H.F. and Brorsen, M., 1978.
On the design of gravity structures using wave spectra.
Lecture on Offshore Engineering, Edited by W.J.Graff and P. Thoft-Christensen, Institute of Building Technology and Structural Engineering, Aalborg University, Denmark.

Burcharth, H.F. og Larsen, Torben., 1988.
Noter i Bølgehydraulik.
Laboratoriet for Hydraulik og Havnebygning, Aalborg Universitet.

Burcharth, H.F., 1991.
Bølgehydraulik.
Department of Civil Engineering, Aalborg University.

Dean, R.G. and Dalrymple, R.A., 1991.
Water wave mechanics for engineers and scientists.
Second printing with correction, World Scientific Publishing Co. Pte. Ltd., Singapore.

Frigaard, P., Helm–Petersen, J., Klopman, G., Stansberg, C.T., Benoit, M., Briggs, J., Miles, M., Santas, J., Schäffer, H.A. and Hawkes, P.J., 1997.
IAHR List of Sea State Parameters – an update for multidirectional waves.
IAHR Seminar Multidirectional Waves and their Interaction with Structures, IAHR Congress, San Francisco.

Goda, Y., 1985.
Random seas and design of marine structures.
University of Tokyo Press, Japan.

Holthuijsen, L. H., 2007.
Waves in Oceanic and Coastal Waters.
Cambridge University Press, UK.

Guo, J., 2002.
Simple and explicit solution of wave dispersion equation.
Coastal Engineering, Vol. 45, pp. 71-74.

Hunt, J. N., 1979.
Direct solution of wave dispersion equation.
Journal of Waterway, Port, Coastal, and Ocean Engineering, Vol 405, pp. 457-459.

IAHR Working Group on Wave Generation and Analysis, 1986.
List of Sea State Parameters.
Published jointly by IAHR and PIANC as a supplement to the PIANC Bulletin, January.

Klopmann, G. and Stive, M.J.F., 1989.
Extreme waves and wave loading in shallow water.
E & P Forum, Report No. 3.12/156.

Kofoed, J.P., 2000.
Optimization of Overtopping Ramps for Utilization of Wave Energy.
Report for the Danish Energy Agency, J. No. 51191/98-0017,
Hydraulics & Coastal Engineering Laboratory, Aalborg University, Nov. 2000.

Liu, Zhou and Frigaard, Peter, 1997.
Random Waves
Department of Civil Engineering, Aalborg University.

Neu, H.J.A., 1982.
11-year deep water wave climate of Canadian Atlantic waters.
Canadian Tech. Rept. of Hydrography and Ocean Sciences, 13.

Newland, D.E., 1975.
In introduction to random vibrations and spectral analysis.
Longman, London, 1975.

Ochi, Michel K. 1998
Ocean Waves - The Stochastic Approach
Cambridge University Press, Cambridge. ISBN: 0-521-56378

Sawaragi, T. 1995
Coastal Engineering – Waves, Beaches, Wave-Structure Interaction
Elsevier, The Netherlands. ISBN: 0-444-82068-X.

Stive, M.J.F., 1986.
Extreme shallow water conditions.
Delft Hydraulics, Intern Report H533.

Sommerfeld, A., 1896.
Theorie mathematique de la diffraction .
Mathematische Annalen, Vol. 47.

Svendsen, Ib A. and Jonsson, Ivar G.,1980.
Hydrodynamics of Coastal Regions.
Den Private Ingeniørfond, Technical University of Denmark, Lyngby. ISBN: 87-87245-57-4.

Wiegel, Robert L.,1964.
Oceanographical Engineering
Prentice–Hall, Inc / Englewood Cliffs, N.J., London.

Young, I.R., 1999
Wind Generated Ocean Waves.
Elsevier, Kidlington, Oxford 1999. ISBN: 0-08-04331

Appendix A

Hyperbolic Functions

y	y'
$sinh\,\alpha = \frac{e^{\alpha}-e^{-\alpha}}{2} = -sinh\,(-\alpha)$	$cosh\,\alpha$
$cosh\,\alpha = \frac{e^{\alpha}+e^{-\alpha}}{2} = cosh\,(-\alpha)$	$sinh\,\alpha$

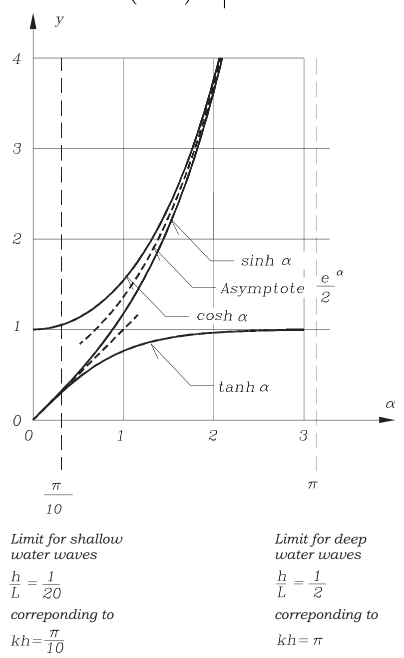

Appendix B

Phenomena, Definitions and Symbols

B.1 Definitions and Symbols

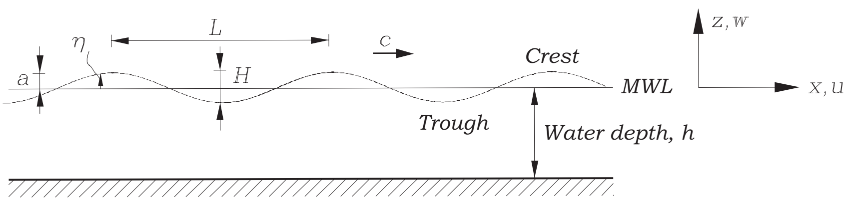

H	wave height
a	wave amplitude
η	water surface elevations from MWL (posituve upwards)
L	wave length
$s = \dfrac{H}{L}$	wave steepness
$c = \dfrac{L}{T}$	phase velocity of wave
T	wave period, time between two crests passage of same vertical section
u	horizontal particle velocity
w	vertical particle velocity
$k = \dfrac{2\pi}{L}$	wave number
$\omega = \dfrac{2\pi}{T}$	cyclic frequency, angular frequency
h	water depth

Wave fronts

Wave orthogonals

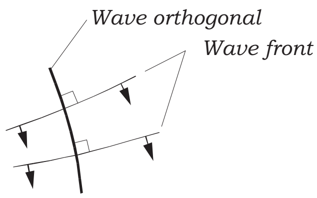

B.2 Particle Paths

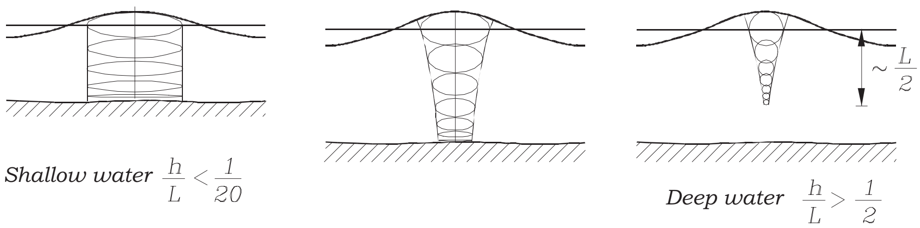

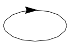 When small wave steepness the paths are closed orbits (general ellipses).

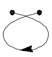 When large wave steepness the paths are open orbits, i.e. net mass transport.

However, the transport velocity is even for steep waves smaller than 4% of the phase speed c.

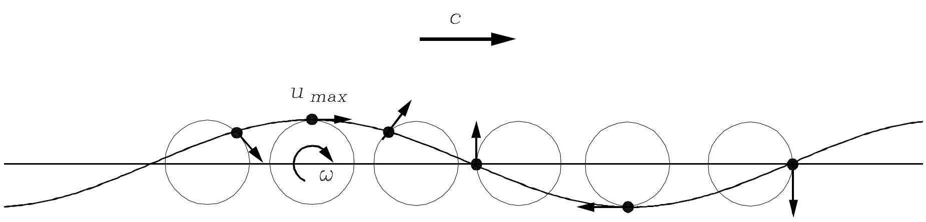

$u_{max} < c$ for deep water waves. For $H/L = 1/7$ we find $u_{max} \simeq 0,45c$

B.3 Wave Groups

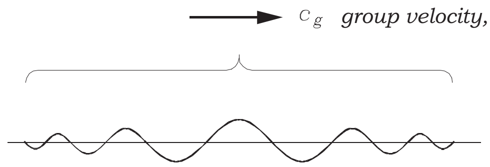

$$c_g = \frac{1}{2} \cdot c \quad \text{for deep water waves}$$

$$c_g = c \quad \text{for shallow water waves}$$

Example:

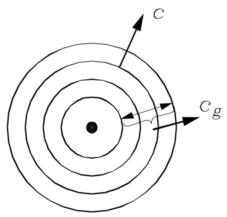

Stone drop in water generates ripples of circular waves, where the individual wave overtake the group and disappear at the front of the group while new waves develop at the tail of the group.

B.4 Wave Classification after Origin

Phenomenon	Origin	Period
Surges	Atmospheric pressure and wind	1 – 30 days
Tides	Gravity forces from the moon and the sun	app. 12 and 24 h
Barometric wave	Air pressure variations	1 – 20 h
Tsunami	Earthquake, submarine land slide or submerged volcano	5 – 60 min.
Seiches (water level fluctuations in bays and harbour basins)	Resonance of long period wave components	1 – 30 min.
Surf beat, mean water level fluctuations at the coast	Wave groups	0.5 – 5 min.
Swells	Waves generated by a storm some distance away	< 40 sec.
Wind generated waves	Wind shear on the water surface	< 25 sec.

B.5 Wave Classification after Steepness

$H/L \to 0$, waves with small amplitude

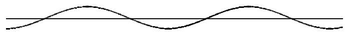

1. order Stokes waves, linear waves, Airy waves, monochromatic waves.

$H/L > 0,01$, waves with finite height

higher order waves, e.g. 5. order Stokes waves.

B.6 Wave Classification after Water Depth

$h/L < \frac{1}{20}$, shallow water waves

$h/L > \frac{1}{2}$, deep water waves

B.7 Wave Classification after Energy Propagation Directions

Long-crested waves:	2-dimensional (plane) waves (e.g. swells at mild sloping coasts). Waves are long crested and travel in the same direction (e.g. perpendicular to the coast)
Short-crested waves:	3-dimensional waves (e.g. wind generated storm waves). Waves travel in different directions and have a relative short crest.

B.8 Wave Phenomena

In the following is described wave phenonema related to short period waves. Short period waves are here defined as typical wind generated waves with periods less than approximately 30 seconds.

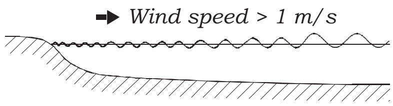

H, L and T increases with increasing wind velocity and the distance the wind has acted over (the fetch).

Wind shear current in the surface layer.

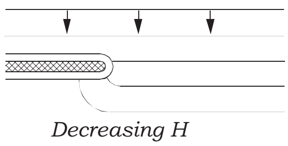

Diffraction

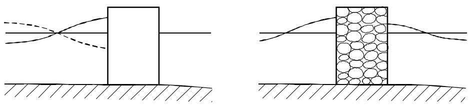

Reflection and transmission

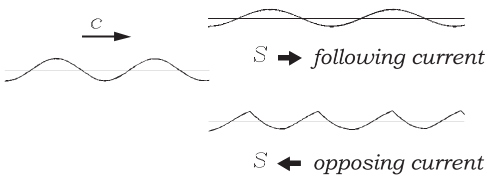

Change of wave form due to current. The corresponding change in phase velocity cause current refraction if S and c are not parallel.

Phenomena related to the presence of the bottom:

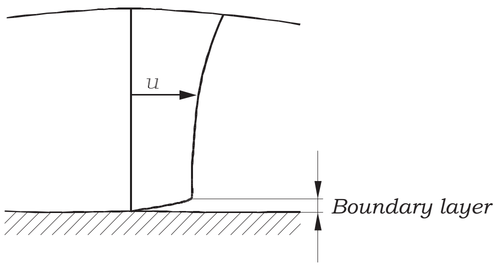

Thin boundary layer due to the oscillating motion. Compare to boundary development at a plate in stationary flow

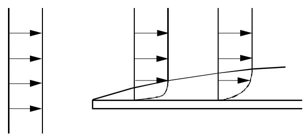

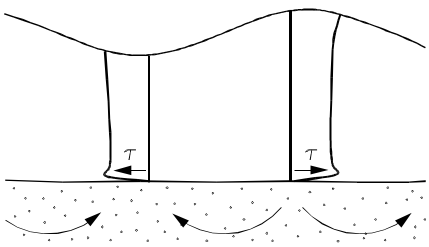

Bed shear stress (can generate sediment transport)

Percolation

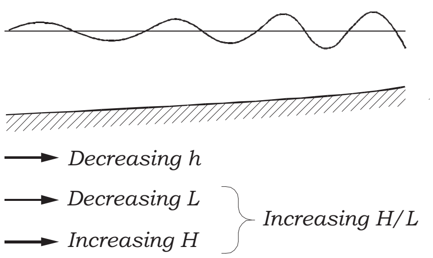

Waves shoal and refract in coastal waters. Refraction when wave crests and depth contours are not parallel

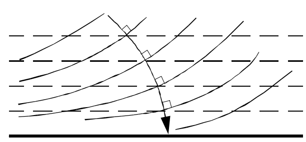

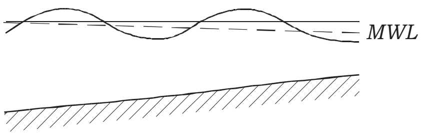

Set-down of MWL before breaker point (typically insignificant)

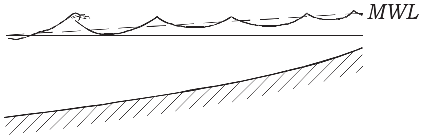

Set-up of MWL as a consequence of decreasing wave height through the surf zone.

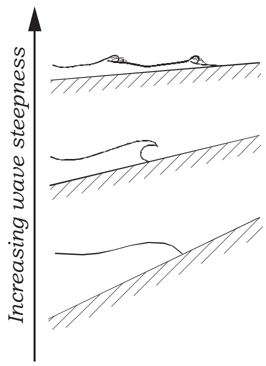

spilling breaker

plunging breaker

Surging

wave breaking in coastal waters when app. $H \geq 0.8h$

Type of breaking depends both on H/L and bottom slope

It should be noted that waves on deep water breaks by spilling when the wind has produced relative steep waves.

Breaking waves generates long-shore currents where the wave orthogonals are not perpendicular to the depth contours.

Appendix C

Equations for Regular Linear Waves

C.1 Linear Wave Theory

$$\varphi = -\frac{a\,g}{\omega}\,\frac{cosh\,k\,(z+h)}{cosh\,kh}\,sin(\omega t - kx) \tag{C.1}$$

$$\eta = a\,cos\theta = \frac{H}{2}\,cos(\omega t - kx) \tag{C.2}$$

$$c = \sqrt{\frac{g\,L}{2\pi}\,tanh\,\frac{2\pi h}{L}} \tag{C.3}$$

$$\begin{aligned} u = \frac{\partial\varphi}{\partial x} &= -\frac{Hc}{2}(-k)\,\frac{cosh\,k(z+h)}{sinh\,kh}\,cos(\omega t - kx) \\ &= \frac{\pi\,H}{T}\,\frac{cosh\,k(z+h)}{sinh\,kh}\,cos(\omega t - kx) \\ &= \frac{a\,g\,k}{\omega}\,\frac{cosh\,k(z+h)}{cosh\,kh}\,cos(\omega t - kx) \end{aligned} \tag{C.4}$$

$$\begin{aligned} w = \frac{\partial\varphi}{\partial z} &= -\frac{Hc}{2}\,k\,\frac{sinh\,k(z+h)}{sinh\,kh}\,sin(\omega t - kx) \\ &= -\frac{\pi\,H}{T}\,\frac{sinh\,k(z+h)}{sinh\,kh}\,sin(\omega t - kx) \\ &= -\frac{a\,g\,k}{\omega}\,\frac{sinh\,k(z+h)}{cosh\,kh}\,sin(\omega t - kx) \end{aligned} \tag{C.5}$$

$$\frac{\partial u}{\partial t} = -a\,g\,k\,\frac{cosh\,k(z+h)}{cosh\,kh}\,sin(\omega t - kx) \tag{C.6}$$

$$\frac{\partial w}{\partial t} = -a\,g\,k\,\frac{sinh\,k(z+h)}{cosh\,kh}\,cos(\omega t - kx) \tag{C.7}$$

$$p_d = \rho\,g\,\eta\,\frac{cosh\,k(z+h)}{cosh\,kh}\ ,\ \text{which at } z=0 \text{ gives }\ p_d = \rho\,g\,\eta \tag{C.8}$$

$$L = \frac{g\,T^2}{2\pi}\,tanh\,\frac{2\pi h}{L} \tag{C.9}$$

$$E = \frac{1}{8}\rho_v g H^2 \tag{C.10}$$

$$P = Ec_g \tag{C.11}$$

$$P = \frac{1}{8}\rho_v g H^2 \cdot (\frac{1}{2} + \frac{kh}{sinh(2kh)}) \tag{C.12}$$

C.2 Wave Propagation in Shallow Waters

$$\frac{H}{H_0} = K_s = \sqrt{\frac{c_0}{c}} \tag{C.13}$$

$$\frac{H^b}{H^{b_0}} = \sqrt{\frac{{c_g}^{b_0}}{{c_g}^{b}}} \cdot \sqrt{\frac{b_0}{b}} \tag{C.14}$$

Appendix D

Exercises

The following exercises are those used for the course in Water Wave Mechanics at Aalborg University. Moreover, there are given some additional exercises for the ardent students in appendix E.

D.1 Wave Length Calculations

Make a computer program to calculate the wave length L.

Start by finding out which parameters the wave length depends on?

Calculate the wave length for the following waves:

- H = 1 meter, h = 10 metre, T = 8 seconds
- H = 1 meter, h = 5 metre, T = 8 seconds
- H = 1 meter, h = 3 metre, T = 8 seconds
- H = 2 metre, h = 10 metre, T = 8 seconds
- H = 2 meter, h = 5 metre, T = 8 seconds
- H = 2 metre, h = 3 metre, T = 8 seconds
- H = 1 meter, h = 10 metre, T = 6 seconds
- H = 1 meter, h = 5 metre, T = 6 seconds
- H = 1 meter, h = 3 metre, T = 6 seconds

The program should also be used for solving the following exercises. Therefore, it is a good idea already now to make the implementation as a function. The function can then be called from a main program for the above given situations.

D.2 Wave Height Estimations

For this exercise we go to the laboratory to measure some regular waves. A pressure transducer is calibrated and placed on the bottom of the wave flume. Afterwards are generated some few regular waves with unknown wave heigh and period. On a PC is a short time series of approximately 20 seconds acquired. The sample frequency is 20 Hz.

The exercise is then to calculate the wave height from the measured pressure time series.

D.3 Calculation of Wave Breaking Positions

We assume a coast profile with constant slope 1:50. Far from the coast we have a water depth of 10 metre. At this position is measured a wave height of 2 metre and a wave period of 8 seconds.

It is assumed that the wave can be described by linear wave theory all the way to the coast line. Moreover, it is assumed that the wave propagate perpendicular towards the coast.

As the wave travels towards the coast and propagate into shallower waters it starts to shoal. The wave is expected to break when the breaking criteria $H/L > 0.142 tanh(2\pi h/L)$ is fulfilled.

- Calculate the water depth where the wave will break.
- Calculate the wave height on the breaking position.
- Calculate the distance to the coast at the breaking position.
- It is now assumed that the wave looses 75% of its energy when it breaks, i.e. the wave height is reduced. Calculate the reduced wave height after the breaking process.
- When the wave breaks there is generated a sandbar. Calculate the position of the following two sandbars.
- When you consider your experiences from beach visits how will you then rate your solution.

D.4 Calculation of H_s

A time series of surface elevations η is available at the course web page.

Download the file and plot the time series. Every member of the group should make a secret guess on the significant wave height. Calculate the average and spreading of your guesses.

Make a computer program that can perform a zero-down crossing analysis. Calculate now H_s from the time series.

Compare the calculated value of H_s with your visual estimations. Do you understand why H_s is used to characterise the wave height.

D.5 Calculation of H_{m0}

You should continue working with the surface elevation time series used for the last exercise.

- Calculate the variance of the signal. What is the unit?
- Calculate H_{m0} as $4\sqrt{variance}$
- Calculate the spectrum
- Calculate the area m_0 of the spectrum
- Explain what information you can get from the spectrum

Appendix E

Additional Exercises

In the present appendix is given some examples on additional exercises.

These additional self-study exercises are on time series analysis.

E.1 Zero-Down Crossing

1) The application of the down-crossing method gives the following 21 individual waves.

wave number	wave height H (m)	wave period T (s)
1	0.54	4.2
2	2.05	8.0
3	4.52	6.9
4	2.58	11.9
5	3.20	7.3
6	1.87	5.4
7	1.90	4.4
8	1.00	5.2
9	2.05	6.3
10	2.37	4.3

wave number	wave height H (m)	wave period T (s)
11	1.03	6.1
12	1.95	8.0
13	1.97	7.6
14	1.62	7.0
15	4.08	8.2
16	4.89	8.0
17	2.43	9.0
18	2.83	9.2
19	2.94	7.0
20	2.23	5.3
21	2.98	6.9

Calculate H_{max}, T_{max}, $H_{1/10}$, $T_{1/10}$, $H_{1/3}$, $T_{1/3}$, $\overline{H}$, $\overline{T}$, H_{rms}

2) Prove $H_{2\%} = 2.23\ \overline{H}$

3) Explain the difference between $H_{1/10}$ and $H_{10\%}$.

4) Suppose individual waves follow the Rayleigh distribution. Calculate the exceedence probability of $H_{1/10}$, H_s and $\overline{H}$.

5) An important coastal structure is to be designed according to H_{max}. The significant wave height of the design storm is $H_{1/3} = 10\ m$. The duration of the storm corresponds to 1000 individual waves.

(1) Calculate $(H_{max})_{mean}$, $(H_{max})_{mode}$, $(H_{max})_{median}$, $(H_{max})_{0.05}$

(2) Now suppose that the storm contains 500 individual waves. Calculate $(H_{max})_{mean}$, $(H_{max})_{mode}$, $(H_{max})_{median}$, $(H_{max})_{0.05}$. Compare with the results of (1).

(3) Use Monte-Carlo simulation to determine $(H_{max})_{mean}$, $(H_{max})_{mode}$, $(H_{max})_{median}$, $(H_{max})_{0.05}$

E.2 Wave Spectra

1) An irregular wave is composed of 8 linear components with

wave no.	1	2	3	4	5	6	7	8
wave height H (m)	5.0	4.3	3.8	3.6	3.3	2.8	2.2	0.3
wave period T (s)	10.3	12	9.4	14	7	6.2	5	3.3

   The recording length is 20 seconds. Draw the variance diagram and variance spectrum of the irregular wave.

2) Convert the variance spectrum obtained in exercise 1) into time series of surface elevation.

3) Make a computer program to simulate the surface elevation of an irregular wave which is composed of 8 linear components. Wave height and period of each component are given in exercise 1). Suppose the sample frequency is 3 Hz and the recording length is 500 seconds.
   (1) Determine H_s and T_s by time-domain analysis.
   (2) Compare the distribution of individual wave height with the Rayleigh distribution.
   (3) Calculate total number of linear components to be given by Fourier analysis N, frequency band width Δf, and the nyquist frequency $f_{nyquist}$.
   (4) Draw the variance spectrum of the irregular wave by FFT analysis. (only for those who have interest.)

4) In reality where $\varepsilon = 0.4 - 0.5$, a good estimate of significant wave height from energy spectrum is

$$H_s = 3.8\sqrt{m_0}$$

   Try to find out the principle of getting this empirical relation.

ISSN 1901-7286
DCE Lecture Notes No. 24